IN VIVO DYNAMIC FUNCTION OF LOWER EXTREMITY HUMAN BIARTICULAR MUSCLES AS MEASURED BY NOVEL ELECTRICAL STIMULATION PROTOCOLS JUXTAPOSED TO COMPUTATIONAL PERTURBATION STUDIES

by

Antonio Hernández

A dissertation submitted in partial fulfillment of

the requirements for the degree of

Doctor of Philosophy

(Mechanical Engineering)

at the

UNIVERSITY OF WISCONSIN-MADISON

2009

UMI Number: 3384118

INFORMATION TO USERS

The quality of this reproduction is dependent upon the quality of the copy submitted. Broken or indistinct print, colored or poor quality illustrations and photographs, print bleed-through, substandard margins, and improper alignment can adversely affect reproduction.
In the unlikely event that the author did not send a complete manuscript and there are missing pages, these will be noted. Also, if unauthorized copyright material had to be removed, a note will indicate the deletion.

UMI®

A dissertation entitled

In Vivo Dynamic Function
of Lower Extremity Human Biarticular Muscles
as Measured by Novel Electrical Stimulation Protocols
Juxtaposed to Computational Perturbation Studies

submitted to the Graduate School of the
University of Wisconsin-Madison
in partial fulfillment of the requirements for the
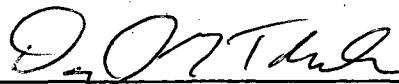degree of Doctor of Philosophy

by

Antonio Hernández

Date of Final Oral Examination: July 29, 2009

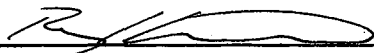Month & Year Degree to be awarded: **December**   **May**   **August** 2009

****
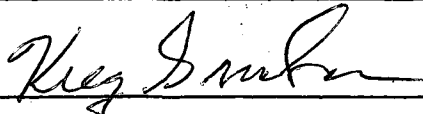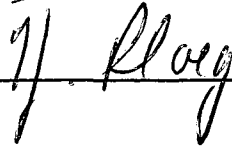
Approval Signatures of Dissertation Committee

Signature, Dean of Graduate School

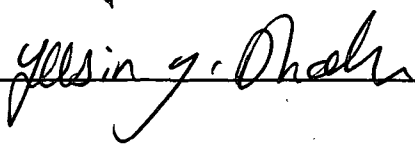Martin Cadwallader   AW

Abstract

Dynamic muscle functions remain elusive in spite of tremendous advances in the areas of computer simulation and dynamical systems analysis. Forward dynamic simulations of movement provide a general description of dynamic muscle function but are dependent on the performance criterion assumed, the complexity of the underlying biomechanical model, and assumptions made regarding properties of the system (segment inertias, joint degrees of freedom, muscle moment arms and passive structures involved). This dissertation presents two electrical stimulation methodologies for the evaluation of dynamic muscle function: one stimulates the limb from a static posture, the other stimulates the muscle during gait. These methodologies are used to assess the dynamic function of the *biarticular* rectus femoris and semitendinosus muscles in walking. The results confirm some of the non-intuitive predictions reached via dynamic simulations but also point out their limitations. More importantly, they inform the biomechanical research community (clinicians and engineers) of the influence of these muscles' normal activity on hip and knee angles during phases of the gait cycle, while acknowledging the possibility that the electrical stimulation paradigm may have some limitations of its own.

Dedication

To

My wife

Nora Mendoza Rivera

ALSO DEDICATED TO:

Maria M. Román Torres, my mother,

Antonio Hernández García, my father,

Mary Milly, Carlito, Yadi, Gibrant and Gretchen, my siblings,

and Lola E. M. Hernández Mendoza, my daughter.

I love you all!

Acknowledgments

I would like to formally thank:

Darryl G. Thelen, Ph.D., for the wise advice he provided to me over the last five years. Your clarity of thought, alertness to opportunities, and overall positivism are greatly appreciated! They assisted me just as much as your technical know-how and financial support in reaching this important point in my career.

Bryan C. Heiderscheit, P.T., Ph.D., for his guidance on various clinical aspects of this work and his great sense of collaboration. Your supportive attitude speaks much about your commitment to others!

Douglass Henderson, Ph.D. and Kelly Burton, director and coordinator, respectively, of the Graduate Engineering Research Scholars program. The financial support that you provide far understates the contributions that each of you makes each day

to the lives of GERS students. I also take the opportunity to thank each and every GERS student. Your presence during our meetings and activities made my Ph.D. years an enjoyable journey.

Dr. Sanjay Asthana, director of the University of Wisconsin's Institute on Aging (IoA) and all other staff of the IoA, for providing me financial support through a 3-year Biology of Aging and Aging Diseases Training Grant (NIH/NIA T32 AG20013) as well as a place to share my findings. I enjoyed working with you all!

Dr. Deborah McLeish and Dr. James Leonard, both Physical Medicine and Rehabilitation physicians who collaborated with me on my experiments. Thanks for letting me approach you and for lending me your medical expertise.

Yasin Y. Dhaher, Ph.D., Dr. Zev Rymer, and all other staff and students of the Sensory Motor Performance Program (SMPP) at the Rehabilitation Institute of Chicago (RIC) for the opportunity to learn from them. I also received financial support from the RIC-sponsored Midwest Rehabilitation Research Network Grant.

Kreg Gruben, Ph.D., Nicola Ferrier, Ph.D., and Heidi Ploeg, Ph.D., for being members of my Ph.D. Committee and for teaching me valuable lessons in courses that I

took with them. I similarly thank all of the professors I had at the University of Wisconsin-Madison. Thanks to each of you for providing me new knowledge and tools.

All student members, current and past, of the *Neuromuscular Biomechanics Lab* and the *Bone and Joint Biomechanics Lab*, for their friendliness, support, and collaboration. I especially want to thank Dr. Elizabeth Chumanov and Dr. Amy Silder (both graduating in the same year as me) for their friendship and technical contributions, and undergraduate students Yomary Muñoz and Amy Lenz for their assistance.

All the subjects who participated in my *in vivo* experiments. Thanks for your courage and desire to contribute to this work.

My grandparents, parents, and siblings, who have loved and supported me throughout my life. I reciprocate your love.

My in-laws, América Rivera and Andrés Mendoza, who are much like second parents to me. I am honored and very proud to be your son-in-law!

My wife and daughter, for giving new meaning to my life and bringing so much joy into it! You are my dearest loves.

God, for all the blessings bestowed upon me, including all the people in this list.

Table of Contents

List of Tables

List of Figures

Chapter 1

Introduction

1.1 Background

For centuries, physiologists, biomechanists and clinicians have attempted to understand muscle functions. Looking at the orientation of the muscles with respect to the joints and the muscles' force producing characteristics, father of biomechanics Giovanni Alfonso Borelli first described the human musculoskeletal system as an arrangement of levers that provided a mechanical means of moving the body and exerting forces on external objects [1]. This view of the body as a biomechanical system gave rise to the field of biomechanics. Still, nearly 330 years after the publication of Borelli's De Motu Animalium, we do not fully understand muscle functions, especially those of the biarticular muscles.

In the modern view of the musculoskeletal system, muscles span the joints across movement directions (or degrees of freedom). Depending on which side of the axis of a rotational degree of freedom a muscle is, it then receives an adjective to describe its function. In this manner, muscles may be described as flexors, internal rotators or adductors when they are on one side of a joint axis, and extensors, external rotators, and abductors if they are on the other side of the joint axis. Based on these definitions, all muscles of the body have been characterized according to their anatomical orientation with respect to the joints they span. Muscles acting along the same direction in a joint have been named agonists and those acting in opposite directions have been named antagonists. In the United States, this classification of muscles is taught to medical doctors, physical therapists, and most other health professionals, often during their first year of professional training.

During the last 20 years, it has become clear that the view of muscles as simply acting to accelerate the joints they span is too limited. The implication of the body being a multi-body linked segment system has been brought to the foreground; namely, that muscles acting to accelerate a joint would also accelerate all other joints of the body due to the reaction forces that spread throughout the skeleton [2]. Reaction forces acting at the distal end of a segment would tend to rotate the segment about its proximal joint. Hence, a uniarticular

muscle volitionally acting to accelerate a particular joint would also accelerate other joints, a phenomenon called *dynamic coupling* in the field of mechanics. Furthermore, this phenomenon gives rise to the possibility that a biarticular muscle—one spanning two joints—could accelerate one of its spanned joints in a direction opposite to its anatomical orientation there. Therefore, neither the magnitude nor the acceleration that a biarticular muscle imparts to a particular joint in the body can be simply inferred based on anatomical observation alone. These values must be determined after consideration of the inertial properties of the body segments, the body posture at the moment that the muscle is active, and the external forces acting on the body [3]. During human movements, when the posture of the body is changing over time, the function of a muscle should thus be considered *dynamic* [4].

The many complexities of the body anatomy and physiology fueled the rise of computational biomechanical models of the human body in the late 20th century. Computer-generated models proliferated as their ability to incorporate the geometry of the body and computational dynamics engines developed [5]. One of the challenges to inferring muscle function from actual motion is accurately measuring the true movements, such that the models can be solved for the muscle forces that generated them. As marker-based,

high-speed motion capture systems became available, it was possible to have fairly accurate motion data to feed to the model. The methods of inverse kinematics and inverse dynamics, first developed by roboticists, were used to back-calculate the joint angles present out of segmental marker trajectories, and the joint torques necessary to produce such motions. But the sub-systems studied were often indeterminate—i.e., having more muscles than required to actuate a joint in a particular direction. Fortunately, methods have been devised to solve the redundancy problem via the incorporation of optimization criteria [3]. Of course, these optimization criteria involve assumptions about what the muscles are trying to optimize during the performance of tasks, and the solutions achieved in this manner are still subject to debate [6].

Dynamic models can also be driven in a forward manner, starting with assumed muscle forces. Due to dynamic system instability, forward driven models are often required to track a specific motion. By assuming a performance criterion and iterating on the solutions, it is possible to arrive at an optimal set of muscle excitations that produces a given motion [3]. Further, a system dynamics-based approach has been developed that can converge on the measured kinematics in a fraction of the computational time, making the generation of subject-specific forward dynamic simulations more widespread [7]. The

forward dynamic simulation method can also be used to predict muscle function during specific tasks by perturbing a specific muscle excitation pattern and seeing how the perturbation affects the motion of the joints [8, 9].

In recent years, many simulation studies have been performed that attempt to elucidate either the contributions of muscles to normal movements or to specific pathologies. A few examples of applications where this approach has been used are in determining the contributions of muscles to the motions of the body segments or center of mass during the swing [9, 10] and stance [11-14] phases of normal walking, to stiff-knee [9, 15, 16] and crouch [17] gaits in cerebral palsy, and to post-stroke hemiparesis [18]. One of the challenges of using the techniques is that models of different complexities seem to yield different results [19, 20]. Different authors with similar methods have arrived at different conclusions regarding the contributions of specific muscles to movement. In addition, due to dynamic coupling, some of the predicted functions are contrary to clinicians' learned understanding of muscle functions. As a result, the dynamic functions of muscles have not yet been agreed upon.

1.2   Scope and Contribution of this Dissertation

There are many applications to understanding muscle function—investigating the neural control of movement, the treatment of movement pathologies, and the improvement of sports performance, to name a few. My particular area of interest is the treatment of gait impairments. In this realm, importance is placed on understanding the specific contributions of muscles to movement, such that one may predict the deficits that would arise when a muscle is impaired, or the ways in which the muscles can be used to compensate for impairments elsewhere—such as in the joints or in other muscles. From a clinician's perspective, therefore, it is critical to validate the muscle function predictions of forward dynamic simulations, and to put these predictions in a context that is clinically relevant—for example, when a model states that a muscle induces knee extension acceleration at a specific point in the gait cycle, what does that mean in terms of the ensuing motion? And how is the motion affected if that muscle's activity is increased or decreased? These are the types of questions that are explored in this dissertation. Figure 1.1 illustrates the contribution of this work via a specific example.
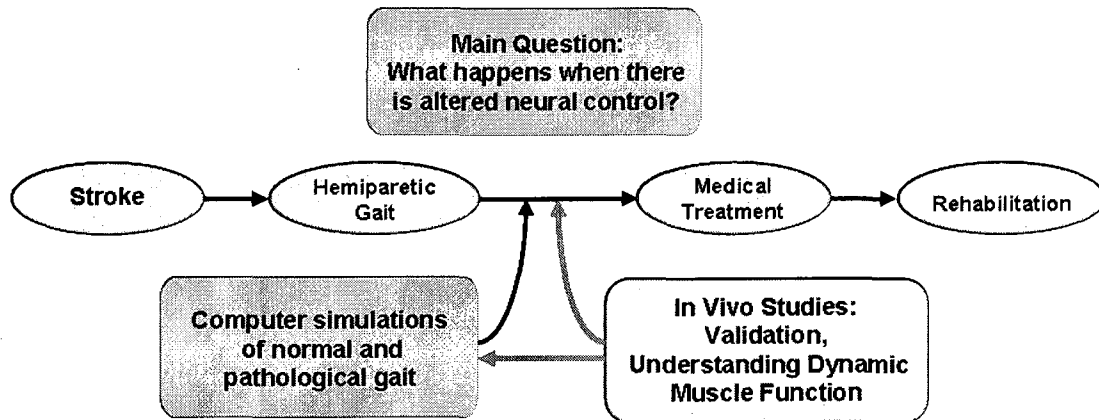
Fig. 1.1: Example of the contribution of this work.

The goal of post-stroke gait rehabilitation treatment is to provide subjects with improved functional performance after a neural insult. The ovals in the figure indicate the normal path followed by a stroke patient in his/her way toward rehabilitation. The problem is that an important question remains unanswered: what are the gait changes that occur when there is altered neural control? Biomechanics labs are producing computer simulations of normal and pathological gait to help answer this question. The current work contributes in-vivo studies to validate the predictions of dynamic simulations as well as clinical interpretation of those predictions in terms of the induced motions.

The specific focus of this thesis is on the biarticular muscles of the lower extremity. These muscles are particularly difficult to understand because, as stated in the Background, they have the potential to accelerate one of the spanned joints opposite to what one would assume based simply on anatomical observation. For example, the rectus femoris has traditionally been thought of as a hip flexor and knee extensor. However, simulations have suggested that this muscle is a hip and knee extensor around the point when the muscle is normally active during gait [10]. Treatment of spastic stiff-legged gait often involves the transfer of the rectus femoris insertion point on the patella to an alternate location (either

medially to the sartorius tendon or laterally to the iliotibial band) to avoid the knee extension moment that it generates while retaining its "flexor" function at the hip [21]. While rectus femoris transfer effectively reduces this muscle's moment arm at the knee, it may not contribute to hip flexion acceleration. As a consequence, the treatment decision may be compromised by a lack of understanding of dynamic muscle function.

Another example of the difficulty in understanding biarticular muscle function can be found in the hamstring muscles. Positioned on the back of the femur, these biarticular muscles are anatomically configured as hip extensors and knee flexors. However, in a study of the contributions of muscles to walking, it was found that the hamstrings could be contributing to knee extension during stance [17]. In addition, at the moment that this muscle is normally active in swing, it may be a hip flexor [10].

Until recent times, there had not been a scientifically sound methodology to test dynamic muscle function in vivo. Two paradigms to study muscle function in vivo existed: in one paradigm, a specific muscle was injected with botulinum toxin to reduce its activity during a task and the motion produced in the absence of this muscle's activity was compared to normal motion [22, 23]. In the second paradigm, the muscle was electrically stimulated and the effects of muscle activity on generated torques was recorded [24]. Disadvantages of

the first paradigm are that it eliminates muscle activity throughout the entire gait cycle (not just at the time when it is to be studied) and that the muscle properties may be altered by the injection [25]. A disadvantage of the second paradigm is that motor unit recruitment may be different during electrical stimulation than during normal muscle activity. However, this shortcoming might be less important if we are only interested in the macro motion of the limb or body, i.e., what happens to the skeleton as an incremental force is applied at the muscle origin and insertion points? An advantage of this second paradigm is that it allows for application of the stimulus at specific points in the gait cycle (e.g., at the time when it is normally active, or at a time when the muscle is suspected to be spastic in pathology). What the authors of this paradigm did not do was to apply the stimulation during movements.

In collaboration with the Rehabilitation Institute of Chicago, we devised an initial experiment to measure *in vivo* muscle function starting from static postures by extending the electrical stimulation paradigm to allow motion of the lower extremity [26]. We have more recently developed a second methodology to measure dynamic muscle function *in vivo* during walking. Both methodologies stimulate the muscle for only a brief period of time (90 ms) and measure the response quickly (within 300 ms), limiting the potential for other muscles to contribute to the motion via reflex activity. The advantage of the first

methodology is that it reduces variability by fixing the pelvis in space and focusing on the lower limb alone while removing many of the assumptions involved in the simulations. The advantage of the second methodology is that it analyzes motion during walking and that it makes no restrictions on possible movements (e.g., fixing the pelvis or limiting the analysis to two dimensions). By testing muscles in their normal physiological environment while performing their routine functions, and by controlling the timing and wave characteristics of the stimulus, we believe that we are doing a good job at representing the effect of increased muscle activation in movement. The during-walking methodology provides three contributions to the advancement of the study of dynamic muscle function. First, the methodology can be used to validate or refute the predictions of forward dynamic simulations. Second, the methodology can be used to infer what the true contribution of a muscle's activity to a particular movement is. Finally, the methodology can be used to study the effect of altered muscle function in movement (such as might occur in specific pathologies). This knowledge is critical not only for the fundamental understanding of movement production but also to provide clinicians with a more accurate picture of muscle contributions to task performance that should enable them to make better decisions regarding the treatments of specific gait impairments.

1.3 Dissertation Outline and Major Results

This dissertation contains four chapters. Chapters 2 and 3 are two articles that have been published in peer-reviewed journals. Chapters 4 and 5 are the materials for two articles that will be submitted for publication this year.

Chapter 2 is a study of older adult gait entitled: *"Effect of age on center of mass motion during human walking"*. This article documents the changes that occur in the ground reaction forces as people age, explaining how previously observed age-related kinetic changes affect walking performance. The main conclusions from this study are that older adults use the leading limb during midstance to compensate for reduced vertical support and work done by the trailing limb during double support, and that older adults have a reduction in the magnitude of their mediolateral accelerations. This study is relevant to the dissertation because it provides a general description of walking control and an introduction to how changes in muscle activity can influence ground reactions. During our analysis of semitendinosus (ST) dynamic muscle function, we will see that the ST has the potential to modulate the anteroposterior ground reaction force and, therefore, to play a role in gait compensations. The clinical implications of this study are in the understanding of balance and in fall prevention for older adults.

Chapter 3 is a study of dynamic muscle function entitled: *"In vivo measurement of dynamic rectus femoris function at postures representative of early swing phase."* This chapter introduces the first methodology that was developed to measure dynamic muscle function. The main conclusions from this work are (1) that the rectus femoris accelerates the hip and knee into extension at static postures representative of pre-swing and early swing, (2) that the ratios of hip-to-knee accelerations at these postures were reasonably well predicted by a dynamic musculoskeletal model, and (3) that the effects of simultaneous muscle activity of the rectus femoris and vastus lateralis can be found by superimposing their individual effects. This study constitutes the first in-vivo validation of the counter-intuitive prediction that the rectus femoris accelerates the hip into extension, not flexion, at postures representative of its normal activity. In addition, it offered support for the superposition assumption and the hip and knee moment arm ratios assumed in a widely disseminated generic model of the lower extremity [27] .

Chapter 4 is the first of two studies to directly measure dynamic muscle function *during treadmill walking*. In the first study, subjects received electrical stimulation of their rectus femoris at either 50% (pre-swing) or 60% (early swing) of the gait cycle. The stimuli were introduced over random strides and the effect on hip and knee joint angles were

established relative to baseline data obtained from the previous, non-stimulated strides. The results were compared to those of subject-specific forward dynamic simulations of gait that were similarly perturbed. The main conclusions of this study were that the rectus femoris acts to accelerate the hip and knee into extension during the swing phase of walking and that these effects are larger when the stimulus is introduced during pre-swing than when it is introduced during early swing. The simulations were generally consistent with the experiment but failed to predict well the magnitude of the changes for specific subjects in the early-swing case. This work is highly relevant to the understanding of stiff-knee gait in both spastic diplegia (common in CP patients) and hemiparesis (common in stroke patients). (Note: A presentation of the pilot data for this study received the American Society of Biomechanics President's Award at the 2008 North American Congress of Biomechanics, Ann Arbor, MI.)

Chapter 5 is the second study of dynamic muscle function *during treadmill walking.* In contrast to Chapter 4, this study measured the dynamic muscle function of the semitendinosus during the portion of the gait cycle when this muscle is normally active (from terminal swing to early midstance). The results showed that this muscle acts to flex the knee if stimulated during terminal stance, with little (slightly flexing, slightly extending or zero)

change at the hip.   However, if stimulated during early swing, we did not observe significant

joint angle changes relative to the non-stimulated strides.   As in the previous experiment, the

simulations were able to predict the general trends in the data but were less accurate

predicting the subject-specific values of joint angle changes.   To our knowledge, there is no

previous *in vivo* evaluation of semitendinosus dynamic muscle function in the literature.

The conclusions of this work have implications to the understanding of crouch gait—where

the over-activity of the semitendinosus during stance is believed to induce a flexed knee

posture during stance—and to elderly gait—where the biarticular hamstrings may be among a

group of muscles that compensate for reduced power generation at the ankle.

Chapter 2

Effect of Age on Center of Mass Motion During Human Walking

2.1   Abstract

The objective of this study was to investigate the effects of age and speed on body center of mass (COM) motion over a gait cycle.   Whole body kinematics and ground reactions were recorded for 21 healthy young (21-32 y) and 20 healthy older adults (66-81 y) walking at 80, 100 and 120% of preferred speed.   The limb-induced COM accelerations and the work done on the COM by the limbs were computed.   Despite walking with similar gait speeds, older adults did significantly ($p<0.05$) less positive work on the COM during push-off but then performed more positive work on the COM during midstance. As a result, older adults induced lower tri-axial COM accelerations via the trailing limb and higher vertical COM acceleration via the leading limb during double support.   Older adults also reduced the mediolateral COM acceleration induced by the leading limb during the last third of double support.   The forward and vertical components of the limb-induced COM

accelerations were highly correlated ($p < 0.005$) but were not correlated to the mediolateral component during double support, at any speed. Together, these results suggest that older adults use the leading limb to compensate for reduced vertical support and work done by the trailing limb. Further, older adults seem to adapt their gait patterns to reduce mediolateral COM accelerations. These findings are relevant for understanding the factors that underlie walking performance and lateral balance in old age.

2.2   Introduction

Aging induces a shift in joint power production during walking, with older adults exhibiting reduced ankle plantarflexor power during push-off and increased hip flexor power during late stance or hip extensor power during early and midstance [28-32]. These changes have been detected experimentally whether the young and older adults have walked at equal speeds [30, 32] or the power measures have been adjusted to account for a slower gait speed in the older adults [31]. Further, as walking speed increases, the power differences become larger [29, 32, 33]. Although age-related changes in walking coordination have been documented, the factors that underlie these changes are not well understood. Proposed mechanisms include distal muscle weakness [29, 30] and a loss of flexibility at the hip [33]. Increased difficulty and/or concerns with lateral balance [34-36] may also be contributing

factors. A better understanding of the relative importance of these factors can potentially be obtained by considering how individual limbs influence movement at the whole body level.

At least three simulation studies have investigated the coordination of whole body motion during normal walking [11-13]. Although each study looked at a different combination of segments to represent the bulk of the body mass, their combined results support that the ankle plantarflexors contribute significantly to the center of mass (COM) forward and vertical accelerations during late stance and pre-swing. In view of the reduced ankle power output of older adults during push-off, this result suggests that the sagittal-plane accelerations of the COM during double support may be reduced by aging. It is possible, then, that increased hip extensor power is compensatory [29, 30], providing additional acceleration during single support to maintain walking speed.

Age-related changes in joint kinetics may also influence COM motion in the mediolateral direction. It has previously been established that even healthy older adults experience difficulty controlling mediolateral stability [35]. Walking includes a substantial single support period such that control of mediolateral balance may be an issue [28, 37], particularly when transitioning support from one limb to the other. Interestingly, the age-related decrement in ankle power emerges during the double support period. Thus, it is

possible that observed changes in sagittal-plane joint kinetics could alter the control of mediolateral COM motion. This potential coupling of induced forward and mediolateral COM motion could arise mechanically from linked-segment dynamics [38] or neurally, from motor control synergies [39].

This study was designed to investigate age-related changes in tri-axial (forward, vertical, and medial) COM motion during normal walking. We hypothesized that the older adults would exhibit a decrease in induced COM accelerations and work done via the trailing limb during double support, with compensatory increases in induced COM accelerations and work done by the leading limb. Further, we expected the medial and sagittal-plane accelerations induced by the trailing limb during pre-swing to be coupled to each other. Finally, we expected any observed age-related changes in COM accelerations and work to interact with walking speed, becoming larger as speed increased.

2.3   Methods

Twenty-one healthy young (age 26±3 y, height 1.73±0.11 m, mass 69±12 kg) and 20 healthy older adults (age 72±5 y, height 1.69±0.09 m, mass 69±11 kg) performed five walking trials at 80, 100, and 120% of preferred speed along a 10 m walkway instrumented

with three fixed force plates (AMTI, Watertown, MA) and an eight-camera motion capture system (Motion Analysis Corporation, Santa Rosa, CA). These subjects were a subset of a larger gait study of young and older adults, and details of the experimental setup used can be found in a previous communication [32]. Exclusion criteria for this study included major orthopedic diagnoses (bone fractures, joint fusions or replacements, limb amputations) in the lower back, pelvis and lower extremity; joint pain; cardiac, neurologic or balance impairments; and failure to pass cognitive (24 score on mini-mental state exam) and plantar sensation (perception of a 10-g monofilament) tests. Subjects gave informed consent prior to the study. The test protocol was approved by the Health Sciences Institutional Review Board of our institution.

Force plate data were first used to identify the heel strike time for two consecutive foot landings (vertical force > 10 N), from which the start and end times of a gait cycle (GC) were determined. Ground reaction force data were extracted from the middle 50% (25-75%) of this GC, where no limb was in touch with the ground outside of the force plate region. This period involved the end of a step (step 1, 25%-50% GC) and the beginning of the next step (step 2, 50%-75% GC) on the opposite limb. We set the 0% gait cycle mark at the beginning of step 2. We then shifted the step 1 data forward in time so that its start

would merge with the end of step 2 at the 25% GC mark. This manipulation required changing the sign on the mediolateral component of the ground reactions, resulting in the half gait cycles that were analyzed in this study.

Full body kinematics were measured using 42 passive motion capture markers with 23 of them placed on anatomical landmarks of the pelvis, arms, legs and feet, and the other 19 placed on limb segments to facilitate segment tracking [40]. Kinematic data were used in conjunction with heel strike times to determine walking velocity, step length, step width, mediolateral COM excursion and mediolateral stability. Step time was defined as the time between two consecutive heel strikes. Walking velocity was defined as step length divided by step time. Step width was defined as the mediolateral distance between the average positions of the heel markers of the two feet during their respective stance times. Both step length and step width were normalized to body height. Mediolateral COM excursion was defined as the range of mediolateral motion observed over a gait cycle. Because stability is believed to depend on keeping COM motion within the base of support [36] , the mediolateral COM excursion was divided by the step width to obtain an indicator of mediolateral stability.

Tri-axial COM accelerations were computed by dividing the directional components of the net ground reaction force (sum of the two limb contributions) by body mass, and

subtracting gravity's contribution in the vertical direction. COM velocity and position were then computed by integrating the acceleration curves in each direction [41, 42]. Integration constants were assigned by using the average forward velocity as measured by the pelvis markers, and assuming that the average mediolateral and vertical velocities were zero over a full gait cycle. Net acceleration, velocity and position traces were averaged across five trials for each subject to obtain representative COM motion curves at every speed.

The tri-axial COM accelerations induced by each limb were calculated by dividing the directional components of the individual ground reactions by body mass [41, 42]. Limb-induced COM accelerations and work done traces were then averaged over three phases of the gait cycle: *double support* (when two limbs contacted the ground), *midstance* (when one limb contacted the ground and the forward COM acceleration was negative) and *terminal stance* (when one limb contacted the ground and the forward COM acceleration was positive). We also computed the dot product of the individual limbs' ground reactions and the COM velocity vector at each point in time to evaluate the instantaneous power delivered to the COM. We integrated these quantities with respect to time in order to obtain the external mechanical work done by each limb on the COM [42].

A two factor analysis of variance (ANOVA) with two levels on age (young, old) and three repeated measure levels on speed (slow, preferred, fast) was then carried out for each limb-induced acceleration and work quantity. Post-hoc Tukey comparisons were performed to determine the source of significant age and/or age-by-speed effects by comparing the young and old populations at each of the three speeds. Potential coupling between the directional components of the limb-induced COM acceleration was evaluated by pooling the acceleration data from young and older adults along each direction, and calculating Pearson correlation coefficients for every pair of directional components, both within a limb and between limbs. Significance for all statistical tests (ANOVAs, Tukey comparisons and correlation coefficients) was established at $p < 0.05$.

2.4   Results

2.4.1   Spatiotemporal Measures

Average gait speed, normalized step length, normalized step width, and mediolateral

COM excursions were not significantly different between young and older adults at any speed

(Table 2.1).   Further, the COM excursion/step width ratio, an indicator of mediolateral

stability, was not significant with age.

Table 2.1 Spatiotemporal gait measures of young and older adults.

		Slow speed		Preferred speed		Fast speed	
		Ave (SD)	*p*-Value	Ave (SD)	*p*-Value	Ave (SD)	*p*-Value
Gait speed (m/s)	Young	1.058 (0.100)	0.770	1.326 (0.133)	0.919	1.587 (0.133)	0.533
	Old	1.048 (0.103)		1.322 (0.128)		1.557 (0.154)	
Step length, normalized by height	Young	0.376 (0.028)	0.570	0.415 (0.038)	0.960	0.458 (0.042)	0.830
	Old	0.369 (0.043)		0.415 (0.028)		0.453 (0.039)	
Step width, normalized by height	Young	0.038 (0.016)	0.404	0.041 (0.014)	0.299	0.039 (0.019)	0.255
	Old	0.034 (0.018)		0.035 (0.017)		0.033 (0.017)	
Mediolateral COM excursion (m)	Young	0.030 (0.009)	0.083	0.025 (0.007)	0.101	0.021 (0.005)	0.065
	Old	0.026 (0.008)		0.021 (0.007)		0.018 (0.006)	
COM excursion / Step width	Young	0.517 (0.212)	0.734	0.391 (0.162)	0.566	0.360 (0.140)	0.800
	Old	0.544 (0.291)		0.428 (0.239)		0.374 (0.188)	

2.4.2   COM Accelerations

Older adults walked with different COM acceleration patterns than young adults

during double support   (Fig. 2.1.a).   The older adults showed a tendency for reduced trailing

limb-induced tri-axial accelerations and increased leading limb-induced vertical acceleration during double support (Fig. 2.1.b).

COM Accelerations (m/s²), Fast Walking Speed

Limb-Induced COM Accelerations (m/s²)

a. Subphase of Stance

b. Limb Used and Subphase of Stance
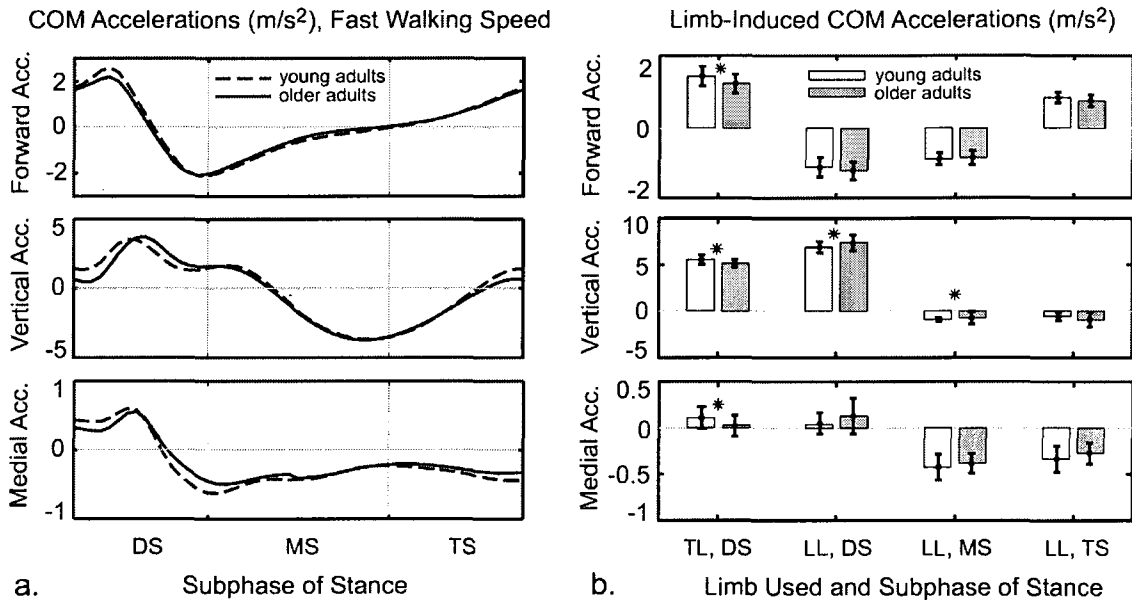
Fig. 2.1. Center of mass accelerations of young and older adults walking at fast speed during stance subphases. (a) Ensemble averaged COM acceleration plots. (b) Average limb-induced COM accelerations. *p-Value < 0.05. Abbreviations: Acc. = Acceleration, DS = double support, MS = midstance, TS = terminal stance, TL = trailing limb, LL = leading limb.

Post-hoc analysis revealed that these double-limb support differences were significant at the preferred and fast speeds (Table 2.2). Generally, the average limb-induced COM accelerations during midstance and terminal stance were not significantly different between the age groups at any speed. The only exception was the leading limb vertical acceleration during midstance, which reached significance at the fast speed.

Table 2.2 p-Values of age and age-by-speed ANOVA effects on limb-induced center-of-mass accelerations and work at each subphase of the gait cycle.

Limb, Subphase	Age p-Value	Age-by-Speed p-Value	Post-Hoc Tukey Comparisons†					
			Slow speed		Preferred speed		Fast speed	
			Difference (m/s^2)	p-Value	Difference (m/s^2)	p-Value	Difference (m/s^2)	p-Value
Forward Acceleration (m/s^2)								
TL, DS	0.062	0.019*	-0.08	0.083	-0.12	0.002*	-0.20	< 0.001*
LL, DS	0.209	0.508						
LL, MS	0.362	0.771						
LL, TS	0.130	0.097						
Vertical Acceleration (m/s^2)								
TL, DS	0.019*	0.051	-0.15	0.273	-0.32	< 0.001*	-0.38	< 0.001*
LL, DS	0.021*	0.066	+0.29	0.020*	+0.56	< 0.001*	+0.53	< 0.001*
LL, MS	0.310	0.023*	-0.02	1.000	+0.09	0.745	+0.24	0.009*
LL, TS	0.114	0.062						
Medial Acceleration (m/s^2)								
TL, DS	0.087	0.036*	-0.03	0.432	-0.06	0.002*	-0.08	< 0.001*
LL, DS	0.188	0.105						
LL, MS	0.287	0.677						
LL, TS	0.078	0.587						
LL, Dec	0.003*	0.031*	+0.09	0.209	+0.13	0.006*	+0.22	< 0.001*
Work (J/kg)								
TL, DS	0.013*	0.021*	-0.02	0.318	-0.04	< 0.001*	-0.06	< 0.001*
LL, DS	0.461	0.695						
LL, MS	< 0.001*	0.014*	+0.04	0.041*	+0.09	< 0.001*	+0.09	< 0.001*
LL, TS	0.120	0.681						

Abbreviations: TL = trailing limb, LL = leading limb, DS = double support, MS = midstance, TS = terminal stance, Dec = medial deceleration phase of double support.

†Change magnitudes (older adults relative to young) and p-values of post-hoc comparisons are included only for those limb-phase conditions where significant age or age-by-speed effects exist.

* p-Value < 0.05.

The trailing limb accelerated the COM forward and the leading limb decelerated it

during double support (Fig. 2.2).
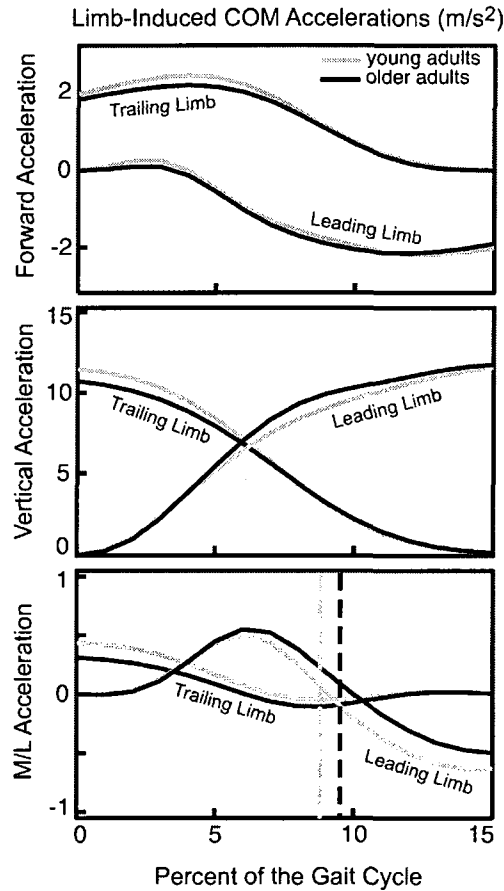
Fig. 2.2: COM accelerations induced by each limb (solid lines) during the double limb support phase for young and older adults walking at fast speed.
The vertical dashed lines show the approximate locations of the mediolateral (M/L) acceleration's zero crossing points for each group.

Older adults showed decreased COM forward acceleration during push-off (first half

of double support) via the trailing limb.   In the vertical direction, the trailing limb reduced its

upward induced acceleration from its maximum value to zero while the leading limb's contribution increased from zero to its maximum value during this phase. Older adults displayed lower vertical acceleration in the first half of double support but greater vertical acceleration in the second half, during leading limb loading. In the mediolateral direction, the trailing limb accelerated the body toward the leading limb during the first half of double support. The leading limb contributed to the COM acceleration toward the new stance side during the first two-thirds of double support, and then accelerated the COM back toward the midline during the last third of double support. The net mediolateral acceleration (sum of the two limb contributions) crossed the zero acceleration line at about 2/3 of the phase for both age groups, representing a functional transition point between mediolateral acceleration and deceleration subphases. Distinguishing between these functional subphases and evaluating the average acceleration over the deceleration subphase yielded a significant reduction in the COM mediolateral deceleration via the leading limb for the older adults at the two fastest speeds (Table 2.2).

2.4.3 Intra- and Inter-limb Correlations

The forward COM accelerations induced by each limb during double support

correlated to the vertical accelerations induced by the same limb (Table 2.3). The mediolateral accelerations induced by each limb during double support did not correlate to either the forward or the vertical accelerations induced by the same limb. The accelerations induced by the trailing limb negatively correlated with the accelerations induced by the leading limb along each direction. These correlations were present at all speeds (Table 2.3).

Table 2.3 Pearson correlations between the COM accelerations induced during double support by the trailing and leading limbs.

Correlated Variables	Slow speed		Preferred speed		Fast speed	
	Correlation Coefficient (r)	p-Value (p)	Correlation Coefficient (r)	p-Value (p)	Correlation Coefficient (r)	p-Value (p)
Intra-limb Correlations						
TL Fwd vs TL Ver	0.471	0.002*	0.509	< 0.001*	0.542	< 0.001*
TL Ver vs TL M/L	-0.180	0.272	-0.164	0.318	-0.259	0.112
TL Fwd vs TL M/L	0.077	0.642	-0.055	0.739	-0.215	0.189
LL Fwd vs LL Ver	-0.491	0.002*	-0.710	< 0.001*	-0.641	< 0.001*
LL Ver vs LL M/L	0.037	0.823	-0.018	0.912	-0.011	0.950
LL Fwd vs LL M/L	0.085	0.609	0.138	0.401	0.063	0.703
Inter-limb Correlations						
TL Fwd vs LL Fwd	-0.663	< 0.001*	-0.635	< 0.001*	-0.606	< 0.001*
TL Fwd vs LL Ver	0.035	0.833	0.197	0.232	0.136	0.410
TL Fwd vs LL M/L	-0.134	0.416	-0.107	0.517	0.160	0.330
TL Ver vs LL Fwd	0.063	0.702	+0.075	0.649	-0.011	0.949
TL Ver vs LL Ver	-0.656	< 0.001*	-0.576	< 0.001*	-0.498	0.001*
TL Ver vs LL M/L	0.010	0.951	-0.030	0.855	0.168	0.308
TL M/L vs LL Fwd	-0.153	0.350	-0.139	0.399	-0.092	0.578
TL M/L vs LL Ver	0.145	0.377	0.160	0.330	0.147	0.371
TL M/L vs LL M/L	-0.810	< 0.001*	-0.798	< 0.001*	-0.816	< 0.001*

Abbreviations: TL = trailing limb, LL = leading limb, Fwd = forward, Ver = vertical, M/L = mediolateral.
* p-Value < 0.05.

2.4.4 External COM Power and Work

The external power and work done by the limbs on the COM exhibited differences

between the age groups (Fig. 2.3). Specifically, the mechanical work done by the trailing

limb on the COM during double support was lower in the older adults than in the young,

reaching significance at preferred and fast speeds (Fig. 2.3.b). The mechanical work done

by the leading limb on the COM during midstance was significantly different between the age

groups at every speed, with midstance work being positive in the older adults but slightly

negative in the young adults (Fig. 2.3.b).
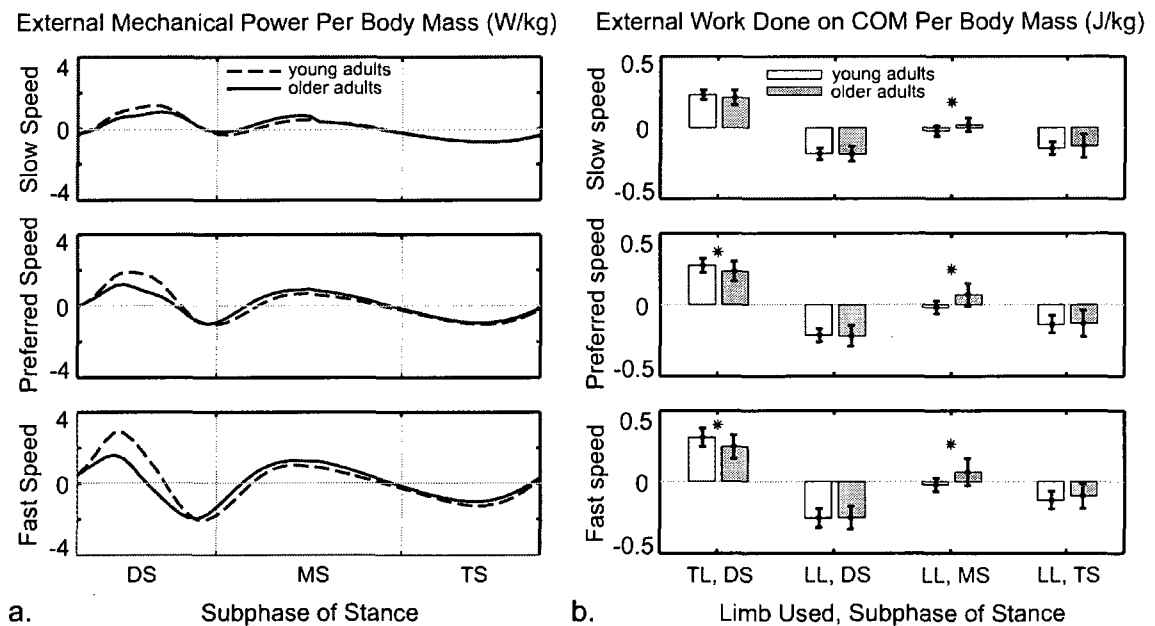
Fig. 2.3: External mechanical power and work done on the body COM during the subphases of stance in young and older adults.

(a) Ensemble averaged power plots. (b) External work done by the limbs. At faster speeds, older adults did less work with the trailing limb during double support. In order to maintain walking speed, the leading limb may compensate by doing net positive work during mid-stance. *p-Value < 0.05. Abbreviations: Acc. = Acceleration, DS = double support, MS = midstance, TS = terminal stance, TL = trailing limb, LL = leading limb.

Both the work done by the trailing limb during double support and the work done by the leading limb during midstance showed discernible age-by-speed effects (Table 2.2).

2.5   Discussion

The older adults exhibited similar preferred walking speed and step length as the young adults at all speeds. However, older adults generated less forward acceleration and performed less work via the trailing limb during double support. Similar to this study, reduced trailing limb work during double support has previously been shown in older adults [43]. These results lead to the question of how a similar walking speed was maintained. Our analyses indicate that compensation was not achieved by the leading limb during double support, since forward accelerations were not significantly different between the groups in this phase (Fig. 2.1.b, Table 2.2). Instead, the older adults performed more net positive work, relative to the young adults, during the subsequent midstance portion of single support. This result is consistent with previous observations of older adults performing more work than young adults via the hip extensor power burst [30, 32], which extends into midstance. Although we did not find significant age-related differences in the forward acceleration when

averaged over midstance, this was the only subphase of the gait cycle when there was a

tendency for slightly greater forward acceleration (i.e., less deceleration) in the older adults

(Fig. 2.1.a). This suggests that the older adults likely coordinated the leading limb during

midstance to functionally compensate for reduced trailing limb push-off during double

support, thereby allowing them to maintain similar walking speeds as the young adults.

During double support (~ 0-15% GC), both limbs are in contact with the ground as

the trailing limb passes responsibility to the leading limb to support and accelerate the body.

We had hypothesized that tri-axial COM accelerations induced by the trailing limb would be

reduced in the older adults during this phase. Our results (Fig. 2.1.b) support this hypothesis.

In the forward and vertical directions, this result is likely due to decreased ankle plantarflexor

power [32]. We also expected that the older adults would then compensate by increasing

vertical support and reducing mediolateral deceleration via the leading limb during this

phase. Indeed, we observed a significant increase in the vertical acceleration in the older

adults, but no significant change in mediolateral deceleration. Upon inspection of the

individual limb contributions to mediolateral acceleration, it can be seen that the leading limb

has a dual role during double support, first assisting the trailing limb to accelerate the body

toward the new stance limb, and then accelerating the body back toward the midline (Fig.

2.2). Dividing the double support phase into mediolateral acceleration and deceleration subphases does indeed result in a significant reduction in deceleration by the leading limb during the deceleration subphase. Based on this finding, we believe that it may be beneficial to define gait phases differently for the mediolateral direction based on the zero-crossings of the COM acceleration curves.

The fact that older adults had reduced mediolateral COM accelerations (relative to the young) during double support suggests that joint kinetic changes in the frontal plane may also exist. In addition, it invites the question whether the older adults may have improved their mediolateral stability by reducing COM excursions while keeping a similar step width [36]. However, the COM excursion/step width ratio was not significantly reduced in the older adults with respect to the young (Table 2.1). Instead, it seems that control of mediolateral accelerations (i.e., the rate at which velocity changes) during the transition from one limb to the other becomes more important as adults age than reducing the excursion/step width ratio. This result suggests that stability measures based simply on COM position relative to foot placement are insufficient to describe the mediolateral balance challenge imposed on the motor control system by walking. Additional dynamic measures

(accounting for mediolateral velocity [44] and/or acceleration) may be needed to fully characterize mediolateral stabilization.

Our investigation of two-way correlations during double support also yielded interesting results. First, we found that the leading limb- and trailing limb-induced tri-axial accelerations were negatively correlated. For example, increased forward acceleration by the trailing limb was associated with increased deceleration via the leading limb. This result may be indicative of mechanical constraints due to step-to-step transitions [42], whereby the lower body configuration with the limbs as two sides of a triangle would tend to generate larger impact forces on the leading limb in response to higher trailing limb accelerations. Hence, the leading limb assists the trailing limb to achieve the forward progression, vertical support and mediolateral shift of the COM. Secondly, we saw that during double support, the forward and vertical accelerations induced by the trailing limb correlated to each other but not to the mediolateral accelerations, consistent with independent lateral control [37]. Therefore, age-related reductions in mediolateral COM acceleration during push-off are likely not attributable to mechanical or neural coupling with sagittal-plane motions. Instead, muscles with the potential to directly induce frontal plane body motions (such as the hip

adductors/abductors on either limb) may be involved in producing this age-related difference [45].

The approach used in this study was able to determine the contribution of individual limbs to COM accelerations and work, but did not directly identify the joints or muscles responsible for those changes. However, it was previously shown in this same older adult population that the work done by the plantarflexors was diminished and the work done about the hips was enhanced, relative to the young adults [32]. Thus, these underlying joint kinetic changes, which are similar to results found by others [28-32], likely contribute directly to the changes in COM kinetics and kinematics observed in this study. It is worth noting that COM accelerations and limb work can be directly computed using only forceplate data [41], which would represent a simpler way than full gait analysis to identify potential age-related changes in gait mechanics.

2.6   Conclusion

In this study, we have shown that healthy older adults control COM motion differently

than young adults when walking at preferred and fast speeds. In particular, older adults rely less on the trailing limb to induce forward and vertical accelerations during double support, and compensate by using the leading limb to increase support and do additional work during midstance. In addition, a significant reduction in the mediolateral COM acceleration occurs that is not coupled to changes in sagittal COM motion. These findings are relevant for understanding the factors that underlie walking performance and the causes of mediolateral balance difficulties in older adults.

Chapter 3

In vivo Measurement of Dynamic Rectus Femoris Function at Postures Representative of Early Swing Phase

3.1   Abstract

Forward dynamic models suggest that muscle-induced joint motions depend on dynamic coupling between body segments.   As a result, biarticular muscles may exhibit non-intuitive behavior in which the induced joint motion is opposite to that assumed based on anatomy.   Empirical validation of such predictions is important for models to be relied upon to characterize muscle function.   In this study, we measured, *in vivo*, the hip and knee accelerations induced by electrical stimulation of the rectus femoris (RF) and the vastus medialis (VM) at postures representatives of the toe-off and early swing phases of the gait cycle.   Seven healthy young subjects were positioned side-lying with their lower limb supported on air bearings while a 90 ms pulse train stimulated each muscle separately or simultaneously.   Lower limb kinematics were measured and compared to predictions from

a similarly configured dynamic model of the lower limb. We found that both RF and VM, when stimulated independently, accelerated the hip and knee into extension at these postures, consistent with model predictions. Predicted ratios of hip acceleration to knee acceleration were generally within 1 standard deviation of average values. In addition, measured responses to simultaneous RF and VM stimulation were within 13% of predictions based on the assumption that joint accelerations induced by activating two muscles simultaneously can be found by adding the joint accelerations induced by activating the same muscles independently. These results provide empirical evidence of the importance of considering dynamic effects when interpreting the role of muscles in generating movement.

3.2   Introduction

Forward dynamic simulations provide a powerful framework to characterize muscle function during movement. For example, simulations of walking have been used to determine the contributions of muscles to joint velocities [10, 46], joint accelerations [8, 47] and vertical support and forward progression of the body [12, 13]. Other investigators have used forward dynamic simulations to evaluate the contributions of muscles in movement disorders, such as stiff knee [15] and post stroke hemiparetic [18] gait. Some of the predictions made using dynamic models challenge commonly held anatomical interpretations of muscle function.

For example, a simulation study suggested that the biarticular rectus femoris (RF), classified anatomically as a hip flexor, induces extension about the hip during the early swing phase of walking. This non-intuitive prediction arises from dynamic coupling between body segments, such that biarticular muscles can induce accelerations in direction opposite to the joint moment they generate [48]. In the case of the rectus femoris, which generates hip flexor and knee extensor moments, the knee extension moment induces an extension acceleration about the hip. When this hip extension acceleration exceeds the hip flexion acceleration generated by the hip flexor moment, the net result is hip extension.

There is a need to assess the accuracy of dynamic models [49] given the discrepancy between anatomical classifications of muscles and model-based predictions of muscle function. Inherent assumptions regarding the geometry [5] and independent action of muscles [50], the representation of joints as kinematic constraints [51] and the consideration of segments as rigid bodies [52] are reasons why the model-based functional predictions could differ from reality. In this study, we used electrical stimulation to empirically test whether the RF could induce hip extension, as previously predicted [10]. Stimulations were introduced at two lower limb postures (toe-off and early swing) that represent phases of the gait cycle when RF activity would be expected during normal walking [53]. For comparison, we also stimulated the

vastus medialis (VM), a uniarticular muscle crossing the knee, at the same postures. We hypothesized that both the RF and VM would extend the hip and knee, but that the relative magnitude of induced hip and knee accelerations would differ between postures and muscles, according to the predictions of a dynamic model. Theoretically, the postural effects arise from the dependency of the system inertia matrix [48] and muscle moment arms [5] on the hip and knee joint angles whereas the muscle effects arise due to RF exerting a hip flexor moment that VM does not. We also tested the hypothesis that superposition, an assumption of most dynamic models, would hold for this two-muscle system, such that the sum of the joint accelerations induced by the muscles' independent actions would be a good approximation of the joint accelerations induced during simultaneous muscle stimulation.

3.3   Methods

3.3.1 Experimental Procedure

Seven young, healthy adults (5 males, 2 females; age 26 ± 2.5 years, height 1.77 ± 0.11 m, mass 71.0 ± 7.8 kg) with no history of musculoskeletal problems or neurological dysfunction provided their informed consent prior to participating in our University of Wisconsin Internal Review Board-approved protocol.
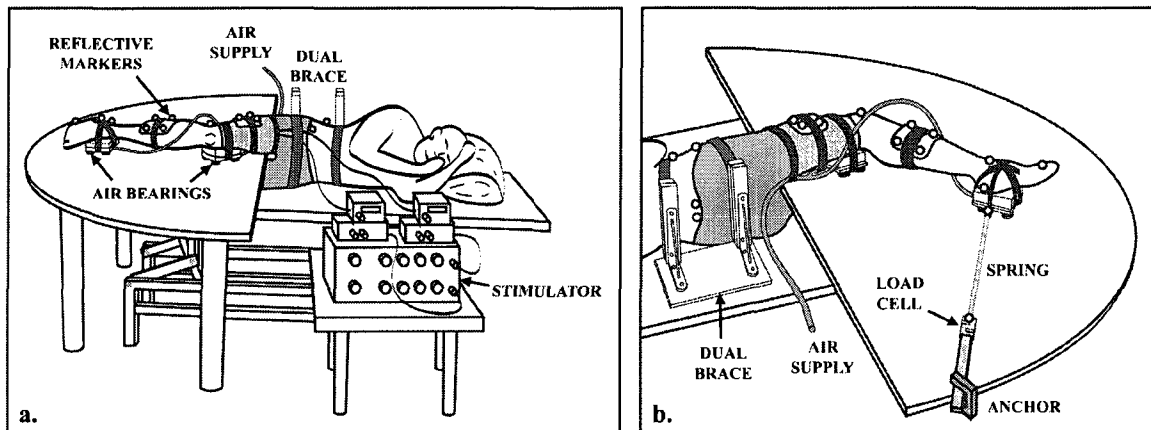
Fig. 3.1: Experimental Setup.

(a) The lower extremity was supported on air bearings that allowed near frictionless motion in the sagittal plane. Pelvis motion was restricted by a dual brace, padded restraint. An electrical stimulator delivered a pulse train to the rectus femoris, the vastus medialis or both muscles simultaneously. Reflective markers were used to measure the induced lower extremity kinematics via an 8-camera motion capture system. (b) Compliant springs, attached to fixed load cells, were used to hold the limb in a desired posture prior to stimulation.

Subjects were positioned side-lying with their right limb supported against gravity via air bearings (Fig. 3.1), allowing nearly frictionless sagittal plane motion. Muscle stimulating and electromyographic (EMG) recording locations were identified based on muscle maps [54]. A dual-channel, current-controlled stimulator (Grass S88, Astro-Med, Inc., West Warwick, RI) was used to induce muscle contractions. Stimulating locations were verified by passing single 300 µs pulses to each muscle of interest (RF, VM) using surface electrodes on alcohol cleaned, gel-primed skin, while slowly increasing the current level until the muscle twitched. The skin was cleaned again and the surface electrodes replaced with

two indwelling stainless steel fine-wires (0.003" bare diameter, A-M Systems, Inc., Carlsborg, WA) for use during testing sessions. EMG signals were recorded at 2000 Hz throughout the trials from RF, VM, vastus lateralis (VL) and the hip adductors (AD) using pre-amplified single differential surface electrodes (DE-2.1, DelSys, Inc, Boston, MA) to assess whether or not the stimulus spilled over to adjacent, non-stimulated muscles.

Testing sessions involved three stimulating paradigms (VM, RF or both muscles simultaneously) and two postures (toe-off and early swing) for a total of 6 experimental conditions. Three trials were performed at each condition, with a single representative trial used in the analysis. Posture order was randomized across subjects, and stimulating paradigms were randomized within subjects. A 90 ms pulse train (four 300 µs pulses at 33 Hz) was used to stimulate muscles. At each posture, the stimulation current for each muscle was adjusted within the range of 1-50 mA to generate visible angular motion at the hip and knee, then kept constant throughout the trials. Compliant springs were connected from one or both of the frictionless carts to fixed load cells (Omega Engineering Ltd., Stamford, CN) to maintain the limb in the desired posture when the muscles were at rest. Due to across-subject variability in passive resistance about the joints, the stiffness of the springs varied from 7 to 63 N/m. Load cell data was used to evaluate the contribution of spring forces to the net joint

moments observed (Fig. 3.1.b). An 8-camera motion capture system (Motion Analysis, Santa Rosa, CA) tracked 15 reflective markers (100 Hz) on the pelvis, thigh, shank and foot. Test trials were also recorded with a video camera.

3.3.2   Dynamic musculoskeletal model

A three segment, two degree of freedom (d.o.f.) musculoskeletal model of the pelvis and lower extremity [5] was used to predict the instantaneous sagittal hip and knee accelerations induced by the RF and VM at the postures of interest (Fig. 3.2.a, 3.2.b). The hip was represented by a hinge and the knee was modeled as a one d.o.f. joint in which tibiofemoral translations were a constrained function of knee flexion angle [51]. The air bearings were assumed frictionless and their masses (0.57 kg each) were added to the inertial properties of the corresponding segments [55]. The muscle paths of the RF and VM were represented by line segments from origin to insertion, with via points used to model wrapping about joints [5].
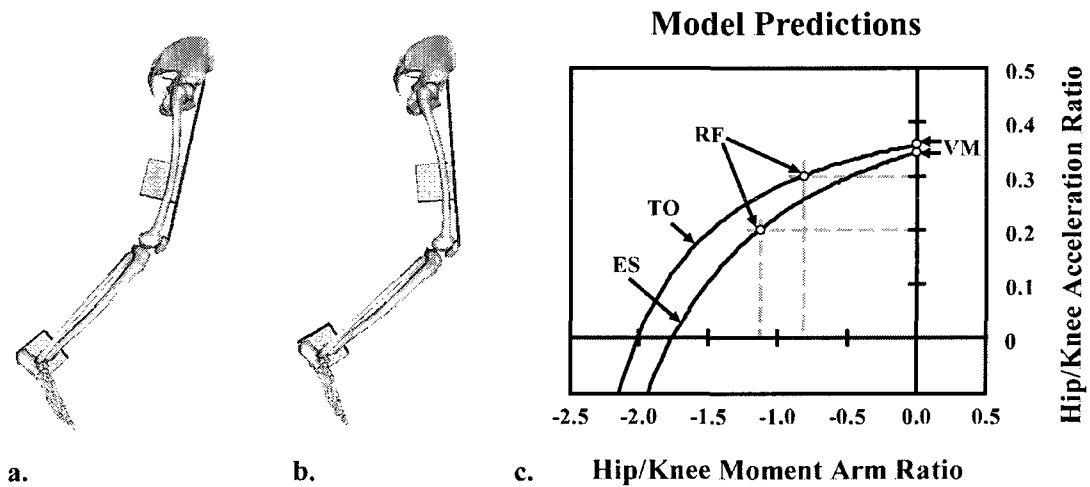
Model Predictions

Fig. 3.2: Two degree of freedom lower limb model at (a) toe-off and (b) early swing phase postures. Rectangular shapes represent the frictionless carts. (c) Our model predicted that both RF and VM induce hip and knee extension at both postures, resulting in positive hip/knee acceleration ratios (circles indicate the model predictions). Higher acceleration ratios are predicted at toe-off (TO curve) than early swing (ES curve) due to postural effects on the inertia matrix (section 2.2, equation 1). The slopes along the curves illustrate the sensitivity of the hip/knee acceleration ratio on the assumed relative moment arms of the muscles about the hip and knee. Flexion is defined as positive in the model.

SIMM Pipeline (Musculographics Inc., Motion Analysis Corp., Santa Rosa, CA) was used in conjunction with SD/FAST (Parametric Technology Corporation, Waltham, MA) to obtain the model's equations of motion, which took the form:

$$\begin{Bmatrix} \ddot{q}_h \\ \ddot{q}_k \end{Bmatrix} = \left[I(q_h, q_k) \right]^{-1} \begin{Bmatrix} r_h^{rf} F^{rf} \\ r_k^{rf} F^{rf} + r_k^{vm} F^{vm} \end{Bmatrix} \tag{1}$$

where q are joint angles, $\ddot{q}$ are joint angular accelerations, r are muscle moment arms, F are

muscle forces, and I is a posture-dependent inertia matrix. Subscripts h and k refer to the hip and knee, respectively, while superscripts rf and vm refer to the muscles included in the model. Gravity-dependent forces are not included in equation (1) since the experiment was conducted in a non-gravitational plane. Velocity- and position-dependent forces are also excluded because the stimulation was introduced while the limb was at rest. The predicted accelerations obtained via equation (1) were then converted into a ratio of hip/knee accelerations which, for an individual muscle, is independent of the muscle force produced. This acceleration ratio was plotted against the hip/knee moment arm ratio to illustrate the dependence of the former ratio on both the inertia matrix (producing a shift in the curves) and the moment arms of the muscles about the joints (causing changes in sensitivity along the curves) (Fig. 3.2.c).

The three segment model of the lower limb was also used to characterize the measured joint kinematics and kinetics. For this purpose, the model was scaled to represent the segment lengths and inertia properties of individual subjects. Body segment coordinate systems, tracking marker locations and segment lengths were first established using the marker positions collected during an upright static calibration trial. Hip joint location was determined via a functional spherical joint center identification algorithm [56]. Hip and

knee angles were computed using an inverse kinematics routine that minimized the sum of squared differences between measured marker positions and corresponding positions on the model. Joint angles were low-pass filtered at 6 Hz (99.5% of the signal power) and numerically differentiated twice to obtain the angular accelerations induced by the stimulated muscle contractions.

3.3.3   Data Analysis

Muscle-induced joint accelerations were defined as the peak accelerations observed within 110 ms following the end of the stimulation train. This time period was chosen to be long enough to accommodate electromechanical delays between stimulation and induced forces, while being short enough to avoid the influence of induced velocities and potential reflex arcs. Acceleration ratios were calculated by dividing the hip acceleration by the knee acceleration at each point in the trials, then averaging the resulting values over a 40 ms period about the point where the product of hip and knee accelerations peaked. The measured hip/knee acceleration ratio for each condition was then determined as the average of the individual ratios across subjects.

The superposition assumption was tested for each joint/posture combination

separately. We added the joint accelerations that resulted from stimulating RF and VM independently (calculated accelerations) and compared them to the measured accelerations in conditions where the two muscles were stimulated simultaneously. We then generated a zero-intercept linear regression through each set of data and inquired whether or not the best-fit line was close to the theoretical relationship (calculated acceleration = measured acceleration) and explained most of the variability in the plot. The first criterion was gauged by comparing the slopes of the theoretical and best-fit lines, since the intercepts in both cases were zero. The second criterion was judged by the coefficient of determination (R^2).

Rectified EMG signals were used to assess which muscles were activated by each stimulation paradigm (Fig. 3.3.a). The first peak in the EMG signal following a stimulating pulse corresponded primarily to stimulus artifact while the second peak was predominantly muscular activation [24]. We empirically determined a time window within the second peak (16 to 23 ms following stimulus onset) where the EMG levels of activated muscles were elevated and always included the maximum. The magnitudes of the individual muscle traces were averaged over this period. Then, the averages of the stimulated muscles were divided by those of the non-stimulated muscles to determine a ratio of EMG activity. Load cell forces were used to compute the joint moments that the springs induced during each trial.
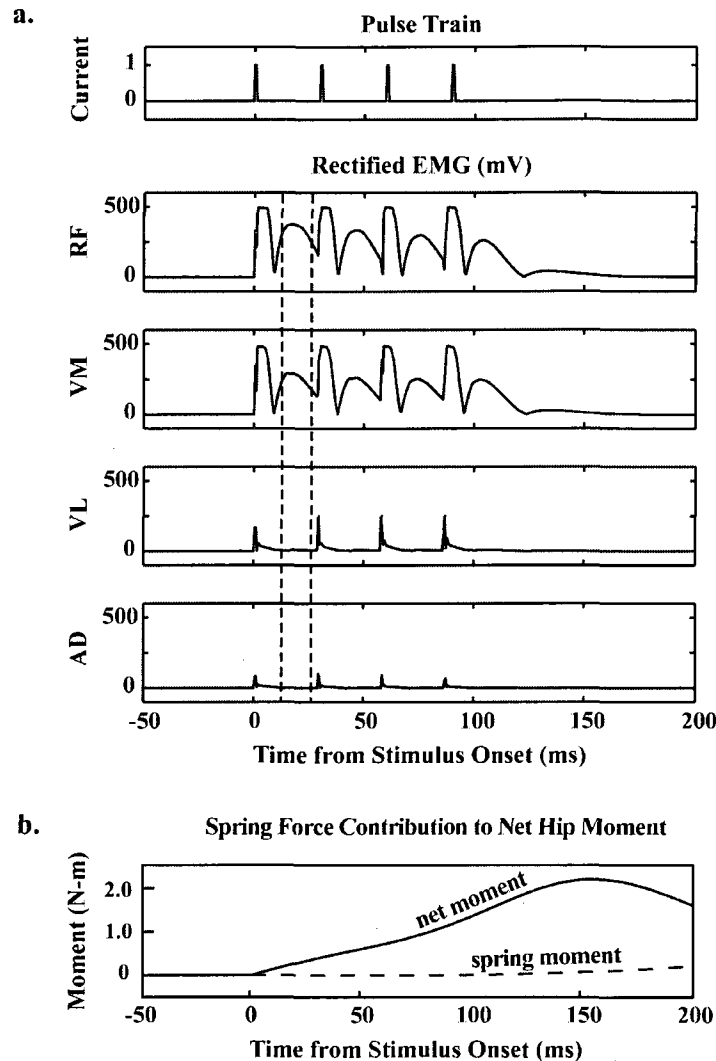
Fig. 3.3: Methods of verification.

(a) Confirmation of proper muscle stimulation. The electrical stimulation pulse train consisted of four 300 μs pulses spaced at 30 ms intervals. The rectified EMG traces of four muscles were monitored over a 200 ms window following stimulus onset. The sharp peaks that occur in the EMG traces with each stimulating pulse correspond to stimulus artifact. The second peaks, seen only in the traces of stimulated muscles (RF and VM in the example above), reflect muscle activation. We compared the average value of the EMG traces in the time window between 13 and 26 ms following the first pulse (dashed lines) to assess whether or not the stimulus spilled over from stimulated to non-stimulated muscles. We also inspected each trace for possible reflex activity. (b) Confirmation of negligible spring-induced joint moments. Spring-induced joint moments and net joint moments were compared to determine the contribution that the springs made to the induced joint accelerations. In both (a) and (b), experimental worst-case results are shown.

These spring-induced joint moments were compared with the net joint moments to confirm that the former did not substantially contribute to the induced joint accelerations (Fig. 3.3.b).

3.4 Results

We found that RF and VM, when stimulated independently, accelerated the hip and knee into extension at both limb postures studied (Fig. 3.4). Video footage of all 7 subjects confirmed this observation (Fig. 3.5). At the toe-off posture, the superposition assumption overestimated the theoretical relationship between calculated and measured accelerations at the hip by 6% and underestimated this same relationship at the knee by 10% (Fig. 3.6.a). At the early swing phase posture, superposition underestimated the relationship at the hip by 13% and overestimated the relationship at the knee by 4% (Fig. 3.6.b). The coefficients of determination between calculated and measured accelerations were high in the toe-off (hip R^2 = 0.82, knee R^2 = 0.80) and early swing phase (hip R^2 = 0.95, knee R^2 = 0.91) postures.
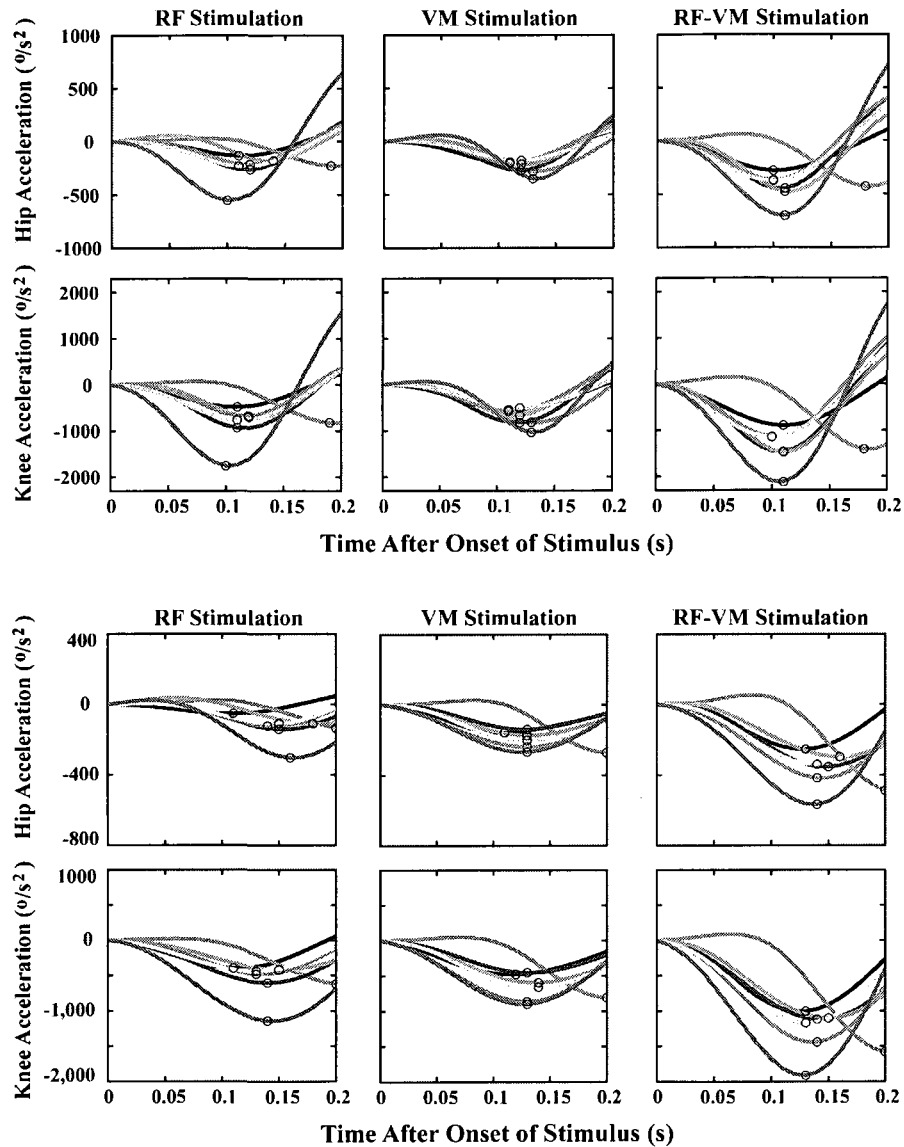
Fig. 3.4: Hip and knee accelerations after stimulation of RF, VM or both muscles simultaneously at (a) toe off and (b) early swing phase posture.

Each curve represents a different subject. Peak induced accelerations over a 110 ms window following the end of the stimulation (i.e. from 90 to 200 ms after the stimulus onset) are highlighted by small circles. Induced hip and knee accelerations were extensor (negative direction) in all cases, and largest for simultaneous muscle stimulation.
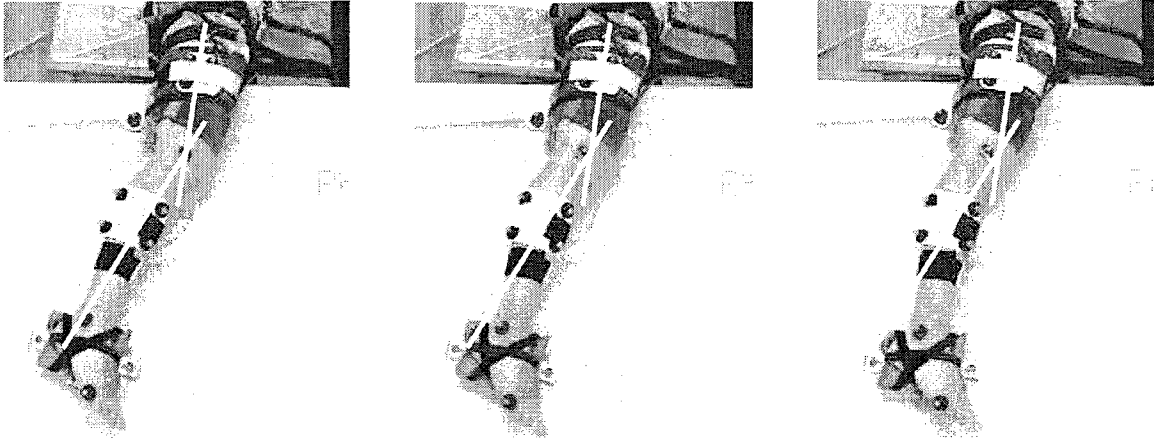
Fig. 3.5: Video sequence of one subject during an RF stimulation trial.

Frames shown are at –40, 40 and 120 ms from the first evidence of movement. A comparison of the limb position against its original configuration (shown by overlaid lines) confirms that both the hip and knee extended. All 7 subjects exhibited similar behavior.

The average (± 1 s.d.) hip/knee acceleration ratios for RF stimulation were 0.29 ± 0.02 in the toe-off posture and 0.24 ± 0.05 in the early swing phase posture. The corresponding values for VM stimulation were 0.34 ± 0.02 and 0.31 ± 0.02. The hip/knee acceleration ratios predicted by the model were within one standard deviation of the measured ratios in all test conditions except VM at early swing phase posture, where the deviation was 1.6 standard deviations (Fig. 3.7). Hence, the acceleration ratios became significantly smaller in going from the toe-off to the early swing phase posture (average change = -0.043, $p < 0.05$).
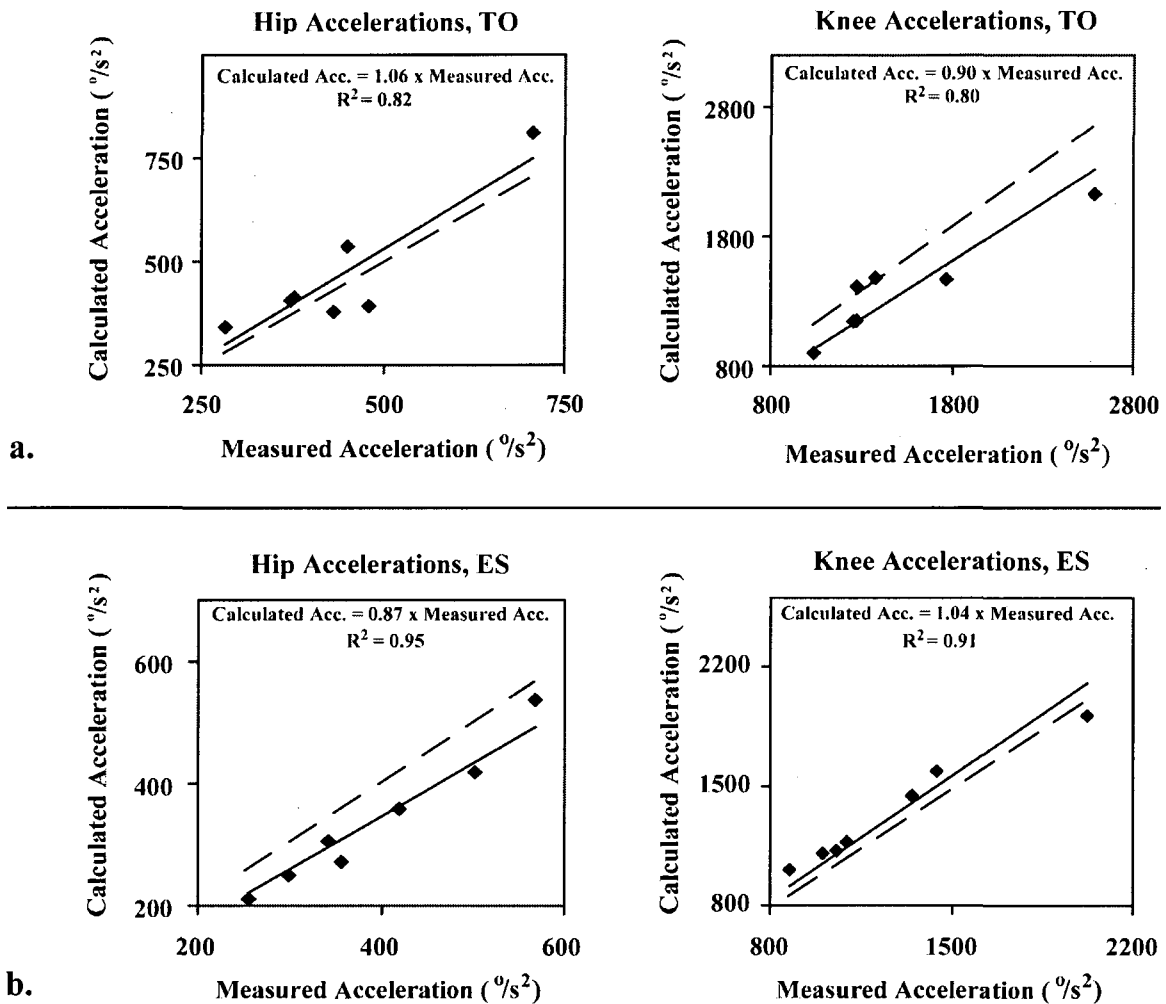
Fig. 3.6: Superposition tests for (a) toe off (TO) and (b) early swing phase (ES) postures.

Each graph is a scatter plot of calculated accelerations (by addition of RF and VM induced acceleration responses) versus measured accelerations (the response to simultaneous stimulation of RF and VM). The theoretical relationship between these two variables, assuming superposition, is calculated acceleration = 1*measured acceleration. Best-fit lines with 0 intercept (solid lines) are compared to the theoretical relationship (dashed lines). Best-fit lines are close to the theoretical relationship (coefficients $\approx$ 1) and coefficients of determination are high ($R^2 \geq 80\%$) in all cases.

Ratio Comparisons
□ Predicted □ Measured

*p < 0.05
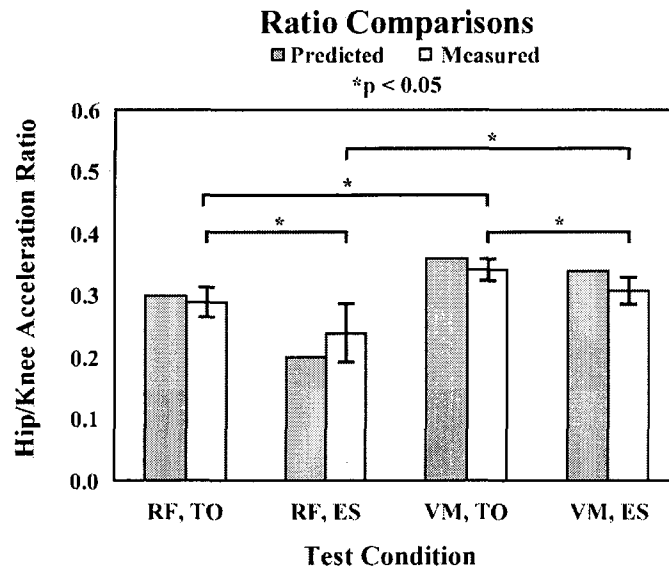
Fig. 3.7: Predicted (light gray) vs. measured (dark gray) hip/knee acceleration ratios.

Measured ratios represent averages across subjects and are shown with ±1 s.d. bars. Experimental differences in the ratio due to changing the posture from toe off (TO) to early swing (ES) were significant (p < 0.05, t-tests) for both RF and VM stimulation and reflect the trends predicted by the model.

The average EMG activity of the stimulated muscles ranged from 22 to 67 times greater than the activity of the non-stimulated muscles during the inter-pulse intervals, suggesting that stimulus spill-over to neighboring muscles was small (Fig. 3.3.a). The net joint moments induced by electrical stimulation of muscles ranged from 1.3 to 10.0 Nm at the hip and from 1.8 to 12.4 Nm at the knee. The spring-induced joint moments were less than 0.2 Nm at the hip and less than 0.1 Nm at the knee. Thus, on average, the spring contribution to the net joint moments was less than 1%, and reached a maximum 4.4% in the worst-case trial among all subjects and conditions (Fig. 3.3.b).

3.5   Discussion

Our results provide experimental evidence of the potential for biarticular muscles to exhibit non-intuitive dynamic function.   Specifically, we showed that RF could accelerate the hip into extension at limb postures representative of toe-off and the early swing phase of gait. This behavior had been predicted based on dynamic simulations [57] but, to our knowledge, had never been measured *in vivo*.   Furthermore, we demonstrated that a two d.o.f., rigid-link dynamic model of the lower extremity correctly predicted experimentally observed posture-dependent changes in the muscle-induced hip/knee acceleration ratio.   Two factors contribute to these changes.   The first factor is inter-segmental dynamic coupling, which refers to the joint accelerations that arise from joint reaction forces [48].   This coupling is modeled mathematically by the system inertia matrix I, which depends explicitly on the hip and knee joint angles (eq. 1).   The second factor is the posture-dependent changes in muscle moment arms that arise from musculoskeletal geometry [5].   For example, the model predicts a large decrease in the hip/knee acceleration ratio for RF stimulation when moving from toe-off to the early swing phase posture, attributable almost equally to changes in dynamic coupling and the muscle's hip/knee moment arm ratio (Fig. 3.2.c).   In contrast, the model

predicts a smaller decrease in the acceleration ratio for VM stimulation, due only to changes in

dynamic coupling (because VM's hip/knee moment arm ratio is always zero). These model

based estimates of the distinct contributions to the acceleration ratio were supported by the

magnitudes of the measured acceleration ratios (Fig. 3.7).

It is important to note that there was also substantial across-subject variability in the

measured ratios (standard deviations, Fig. 3.7), particularly in the behavior of RF at the early

swing phase posture. This subject-dependence of the measured ratios may have been due to

anthropomorphic differences in the hip-to-knee moment arm ratio across subjects. Consistent

with this logic, our sensitivity study showed that the acceleration ratio was more sensitive to

variations in moment arm ratios at the early swing phase posture than at the toe-off posture

(Fig. 3.2.c). These results reinforce the importance of performing sensitivity studies to fully

understand the ramifications of musculoskeletal model assumptions.

The test of superposition revealed how the dynamic functions of muscles combined.

When the induced accelerations of simultaneous RF and VM stimulation were calculated by

superposition and compared to the corresponding measured accelerations, a zero-intercept

linear regression yielded coefficients near 1 under all conditions. In addition, the best-fit line

explained a large percentage of the variability regardless of the posture tested (toe off or early

swing phase) or the joint observed (hip or knee). Thus, our results showed that linear superposition, which has been often assumed in dynamic musculoskeletal models [57-60] and experimental studies [61], was a reasonable approximation of how muscle functions combined in the sagittal plane. Further studies are needed to determine if superposition assumptions hold for other muscles and in non-sagittal directions.

The results of our study cannot be directly used to infer RF muscle function during walking due to the kinematic restrictions imposed. In particular, we restrained the pelvis from moving in this study, whereas muscles have the potential to induce pelvis motion during normal walking. Thus, we cannot assume that the hip joint acceleration will be the same under conditions where the pelvis is free to move. Additionally, we restricted limb motion to the sagittal plane, but walking involves motion in all three directions. Investigations are needed to determine whether the RF and VM, which have greatest moment-generating capability in the sagittal plane, can induce substantial three-dimensional motion of the limb in the unrestricted case. Nevertheless, our study has identified conditions under which the RF can extend the hip. This is an important finding because it demonstrates *in vivo* that biarticular muscles can accelerate one of their spanned joints in a direction opposite to what would be inferred anatomically.

There are also limitations in our ability to measure joint accelerations that should be noted. First, while pelvic motion was restricted passively, a small amount of pelvic motion could potentially occur due to compliance in the restraint system. Secondly, soft-tissue motion, due primarily to induced muscle contractions, could introduce errors when inferring skeletal motion from measured marker kinematics. Finally, the use of numerical differentiation to estimate accelerations can amplify any noise in the kinematic data. Despite these potential shortcomings, visual analyses of video data confirmed the directions of the measured hip and knee accelerations (Fig. 3.5). Furthermore, these directions (Fig. 3.4) and the measured changes in the hip/knee acceleration ratio were consistent across all seven subjects and with model predictions (Fig. 3.7). These results suggest that we achieved reasonably accurate estimates of the muscle-induced joint accelerations.

In conclusion, we have measured non-intuitive dynamic muscle function and postural effects on joint accelerations that are consistent with the predictions of a dynamic musculoskeletal model. These results demonstrate the utility of dynamic models and emphasize the importance of considering dynamic coupling when inferring muscle function during human movement [3, 62].

Chapter 4

Electrical Stimulation of the Rectus Femoris during Pre-Swing Induces Hip and Knee Extension during the Swing Phase of Normal Gait

4.1   Introduction

Stiff-knee gait is a common gait abnormality in individuals with neurological disorders such as post-stroke hemiparesis and cerebral palsy.   Stiff-knee gait is characterized by diminished knee flexion during swing, which is often accompanied by either vaulting or limb circumduction to achieve toe clearance.   Abnormal rectus femoris (RF) activity is frequently implicated as a contributor to stiff-knee gait patterns.   In normal gait, the RF typically exhibits a small burst of activity that spans toe-off [53, 63].   However, in

individuals with stiff-knee gait, the RF often exhibits increased activity during early swing [64, 65] that can arise from spasticity in the muscle. Recent studies have suggested that over-activity in the RF may be present during pre-swing and that this early onset may be at least as important as the activity during swing in causing stiff-knee gait [66, 67].

Dynamic simulations of both normal and stiff-knee gait have been analyzed to better understand the influence that RF activity has on limb motion [9, 10, 16, 46]. These studies indicate that muscle activity prior to toe-off is a key determinant to the amount of knee flexion seen during swing. Further, the models suggest that the RF may induce extension about the hip [10], which is opposite of what is traditionally assumed based on anatomy alone [65, 68]. However, gait model predictions are known to depend strongly on how the body segments [19] and muscles are represented [26], and are also likely influenced by variations in muscle coordination patterns. Such factors are challenging to account for in subject-specific gait models, requiring the use of experiments to more fully understand how muscles function during movement.

Recent studies have introduced electrical stimulation procedures to empirically measure the movement induced by activation of muscles [26, 69-71]. In a previous study, we showed that electrical stimulation of the RF induces hip and knee extension acceleration

when the limb is *statically* positioned in postures representative of early swing phase [26]. The purpose of this study was to investigate *dynamic* rectus femoris function during normal walking using a new electrical stimulation protocol. We hypothesized that RF stimulation during pre- or early-swing would act to increase hip and knee extension during swing, but that the magnitude of induced motion would be greater when stimulation occurred prior to toe-off. Further, we hypothesized that subject-specific gait simulations developed with generic musculoskeletal models could properly predict the direction of RF-induced motion, but would not be able to account for experimental inter-stride and inter-subject variability.

4.2 Methods

4.2.1 Experimental Methodology

Seven healthy young adults (age = 30.7 ± 6.3 yr, mass = 71.2 ± 10.0 kg, height = 1.75 ± 0.06 m) participated in this University of Wisconsin Health Sciences Internal Review Board-approved study. The protocol involved subjects performing 90 s walking trials on a split-belt instrumented treadmill (Bertec Corp.; Columbus, OH) while their right rectus femoris was briefly stimulated during either pre- or early-swing of randomly-selected strides

(Fig. 4.1).

4.2.2 Electrical stimulation synchronized to the gait cycle

A dual-channel, current-controlled stimulator (Grass S88, Astro-Med, Inc., West Warwick, RI) was used to stimulate the right rectus femoris. We first located the motor point of the RF by moving surface stimulating electrodes over the skin until a maximum twitch response was observed. We inserted two indwelling stainless steel fine-wires (0.003" bare diameter, A-M Systems, Inc., Carlsborg, WA) into the muscle at that location (Fig. 4.1). The indwelling electrodes were then used to deliver 90 ms current pulse trains (four 300 μs pulses at 33 Hz) to the RF upon the request of a trigger signal. Stimulation timing was controlled by using a custom LabView (National Instruments, Austin, TX) program to monitor vertical ground reactions under each foot in real time. The forces were used to detect heel strikes, from which the stride duration was calculated based on the average period of the last 3 strides. The controller then triggered the muscle stimulator at either 50% (pre-swing) or 60% (early swing) of the gait cycle. Each subsequent stimulus was introduced randomly between the fifth and tenth stride following the previous stimulation.
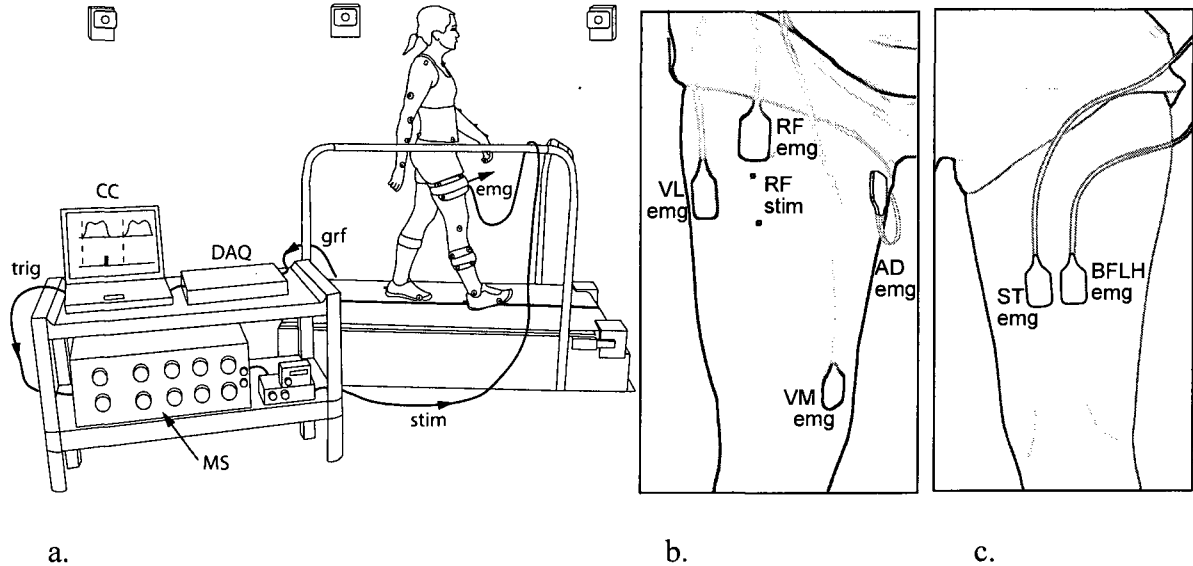
Fig. 4.1: Experimental Setup.

(a) Subjects walked on a split-belt force-plate instrumented treadmill while a computer controller monitored their ground reaction forces. Based on the frequency of heel strikes, the controller estimated the stride period in real time and stimulated the muscle at a pre-specified percentage (50%, 60%) of the gait cycle. The trajectories of the markers changed during the stimulated stride, and these changes were recorded by a high speed motion capture system. Inverse kinematics were used to determine the experimental joint angles. The RF was stimulated using indwelling electrodes, and EMG was recorded anteriorly (b) from the rectus femoris, vastus medialis and vastus lateralis and posteriorly (c) from semitendinosus and biceps femoris long head in order to assess stimulus spillover and reflex activity. CC = computer controller, DAQ = data acquisition unit, MS = muscle stimulator, grf = ground reaction force signals, trig = trigger signal, stim = stimulation train signal, emg = EMG signals to motion capture software, BFLH = biceps femoris long head, ST = semitendinosus, RF = rectus femoris, VL = vastus lateralis, VM = vastus medialis, AD = hip adductors.

4.2.3 Kinematics

Three-dimensional whole body kinematics were recorded at 100 Hz using an 8-camera motion capture system (Motion Analysis, Santa Rosa, CA) to track 44 reflective markers (Fig. 4.1a). Twenty-five markers were placed over anatomical bony landmarks and

the other tracking markers were attached to plates that were strapped tightly to lower limb segments. All kinematic data was low-pass filtered at 6 Hz. Joint angles were computed using a whole body model that included 23 segments and 21 lower extremity degrees of freedom (d.o.f.) to represent the low back, hip, knee and ankle joints [72]. The pelvis was the base segment with 6 d.o.f. Each lower limb included a 3 d.o.f. ball-and-socket representation of the hip, a 2 d.o.f. ankle with non-interesecting talocrural and subtalar joints [5], and a 1 d.o.f. knee where translations and non-sagittal rotations were functions of knee flexion [73].

Segment lengths in the model were first scaled to each subject using anatomical marker positions measured in a standing upright trial. The hip joint center in the pelvic reference frame was then calibrated using a functional joint center identification routine [56]. At each frame of a motion trial, we then used a global optimization inverse kinematics routine to compute pelvic position and joint angles that minimize the discrepancy between measured marker positions and corresponding markers fixed to the body segments [74].

4.2.4 Muscle Activity

Pre-amplified, single differential EMG electrodes (DE-2.1, DelSys Inc., Boston,

MA) were placed on the rectus femoris, vastus lateralis, vastus medialis, semitendinosus,

biceps femoris and adductor muscle group of the right limb (Fig. 4.1.b, c).
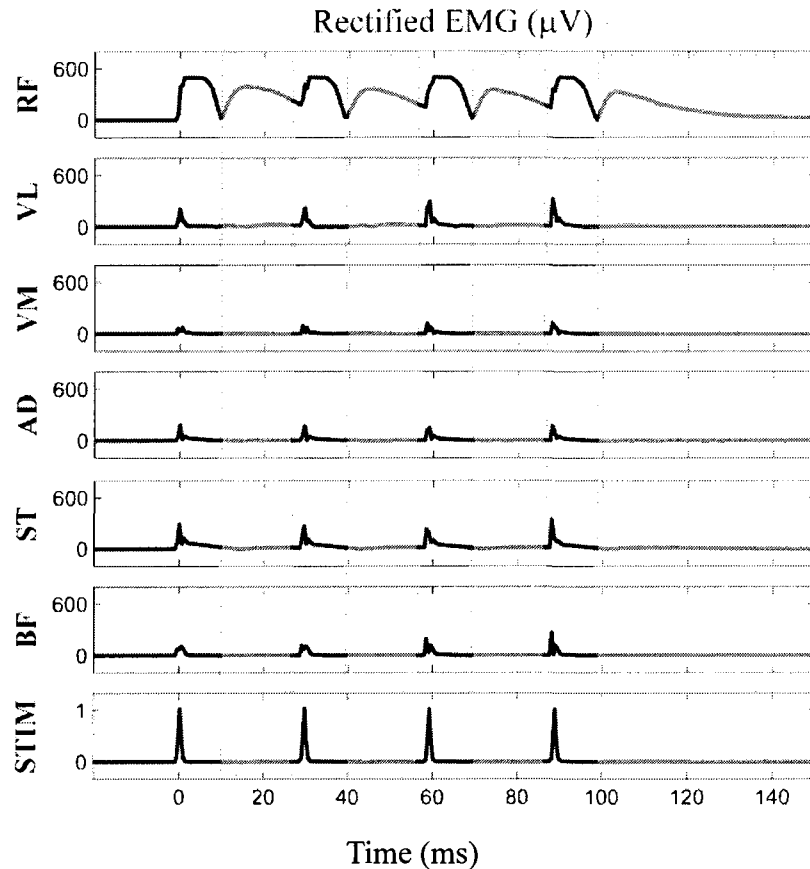
Fig. 4.2: Stimulation current (normalized to 1) and ensuing muscle EMG recordings in μV.
The shaded regions correspond to the regions where the rectified EMG was measured. For each stimulated stride, the central low point in the M-curve following each of the first three pulses was identified and a window created between this point and a point 1 ms from the next pulse. The window for the fourth (and last) stimulus pulse ended at 150 ms to ensure that the stimulus had decayed to zero before looking at potential reflex activity in the subsequent 150 ms window. Abbreviations: STIM = stimulation pulses, BF= biceps femoris, ST = semitendinosus, AD = adductors, VM = vastus medialis, VL = vastus lateralis, RF = rectus femoris.

These EMG activities, the ground reaction forces from the treadmill, and the stimulator's

trigger signal were sampled synchronously at 2000 Hz. The EMG recordings were later

rectified and used to evaluate stimulus spill-over (within 150 ms following stimulus onset)

and potential reflex activity (150-300 ms after stimulus onset) occurring in non-stimulated

leg muscles as a consequence of the electrical stimulation (Fig. 4.2).

4.2.5 Analysis: Periodic prediction model

We employed a periodic prediction model [75] to estimate changes in hip and knee

angles as a result of RF muscle stimulation. The periodic prediction model represents the

normal cyclic nature of movement kinematics and ground reactions during walking by a

linear equation:

$$q(t - \tau) = \alpha + \beta q(t - 2\tau) + \eta(t) \tag{4.1}$$

where q is the joint angle of interest, α and β are slowly varying linear regression

parameters, τ is the stride period, and η is a noise process. That is, a hip or knee joint

angle can be approximated by its value one stride earlier after small offset and drift factors are

accounted for. For each stimulation, we first identified the exact onset (t_o) of the pulse train.

We then computed the cross-correlations of the joint angles between a window that was 90% of an expected stride duration (τ_{exp}) starting at t_0 and corresponding windows of equal size whose starting points varied from 20 ms before to 20 ms after the point $t_o - \tau_{exp}$. The stride period was chosen as that which maximized this cross-correlation. We repeated the process using the two preceding strides to settle on an average stride period τ. We then used linear regression to estimate the parameters α and β relating these two strides. The model was then used to predict the hip and knee angles of both the current (stimulated) stride and the previous (non-stimulated) stride, each based on the stride that immediately preceded it (Fig. 4.3).

The difference between the measured and predicted joint angles were evaluated at the point of predicted peak knee flexion during swing in the stimulated stride. Similarly, the difference between the measured and predicted joint angles was evaluated at a point one period behind. The difference between these two changes was considered to be the effect of the stimulus. The mean effects of the stimulated and corresponding non-stimulated strides of each trial were compared using t-tests to determine if the differences were statistically significant ($\alpha = 0.05$). The experimental effects were also qualitatively compared to the predictions of forward dynamic simulations that were similarly perturbed.

Time (s)
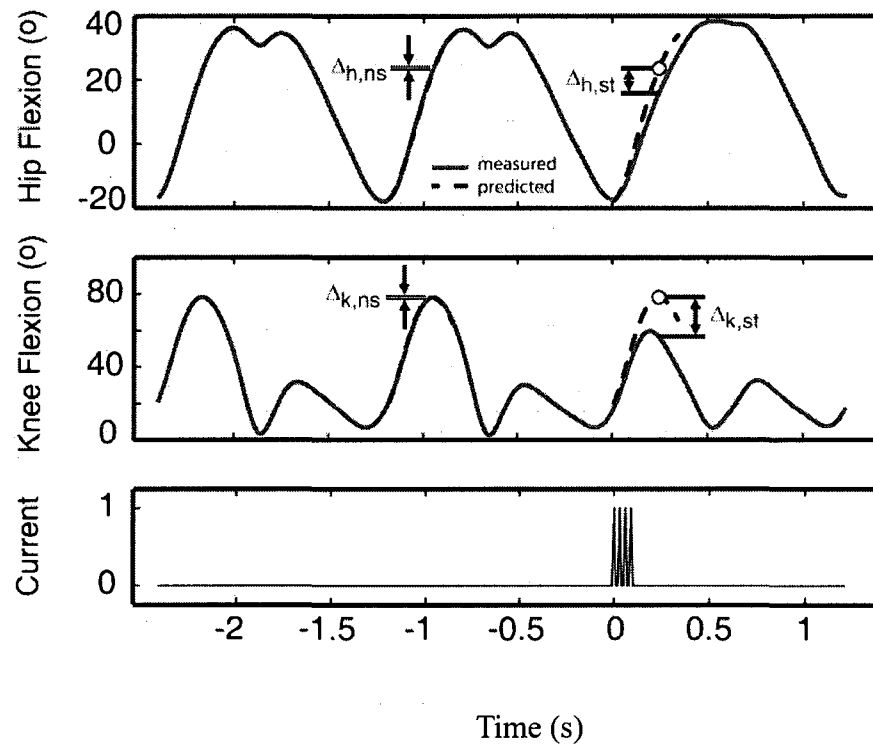
Fig. 4.3. Periodic Prediction Model.

A linear model is constructed based on the two strides preceding the stimulus. This model then predicts expected joint angles for the stimulated stride and the non-stimulated stride preceding it. The measured angle changes between the actual trajectory (red) and the predicted trajectory (dashed black) at the point of predicted peak knee flexion during swing are evaluated for both the hip and the knee. This point is always within 300 ms following the onset of the stimulus. Note that the deviations at the point of peak knee flexion are consistent in direction with the direction that the trajectories are first affected by the stimulus. Hence, we believe these deviations represent the direction of the muscle-induced joint accelerations. Deviations between the actual and predicted trajectories later in time may include the effects of changed posture, reflexes and voluntary muscle activity and were therefore not considered to represent the main effect of stimulation. Δ = joint angle change, h = hip, k = knee, ns = non-stimulated stride, st = stimulated stride. The bottom plot shows the stimulating current pulse train, normalized by its magnitude.

4.2.6 Subject-specific forward dynamic simulations of gait

Scaled whole body models were also used to develop simulations of subject-specific

walking dynamics. We included 92 musculotendon actuators that represented the major muscles acting about the low back, hip, knee and ankle joints [5]. The input to each muscle was an excitation that could vary between 0 and 1. Excitation-to-activation dynamics was represented by a bi-linear differential equation with activation and deactivation time constants of 10 and 40 ms, respectively [76]. A Hill-type musculotendon model was used to describe contraction dynamics [77]. For each subject, we generated simulations of the normal gait stride that preceded a stimulation pulse train. In these simulations, Computed Muscle Control was used to determine a set of muscle excitations that drove the model to closely track measured lower extremity kinematics, while upper extremity kinematics were prescribed to track measured values. This approach has previously been shown to produce simulations of lower extremity joint angles that are within $\sim 1^{\circ}$ of measurements [7]. Excitations were determined that minimized the weighted sum of squared muscle activations [78], which is known to provide reasonable estimates of coordination patterns seen in normal gait [72].

Fig. 4.4: Method of perturbing forward dynamic simulations.

A 100 ms, 0.1 unit increase in the rectus femoris' nominal excitation was introduced at 50% or 60% of the gait cycle. The altered RF excitation and the nominal excitation of the other muscles were applied to the model to generate perturbed forward dynamic simulations. The perturbation-induced changes in hip and knee flexion were recorded.

After generating a nominal simulation, we then perturbed the RF excitation patterns at either 50% (pre-swing) or 60% (early swing) of the gait cycle (Fig. 4.4). This was done by increasing the excitation level of the RF by 0.1 unit (1 corresponds to maximum excitation drive) for a 100 ms period. Changes in the interactions between the stance-limb foot and the ground were characterized by a set of rotational and translational spring-damper units [79]. Hence, the ground reaction forces and moments were allowed to change in response to the perturbations in force, and the effects of these changes were implicitly included in the actions attributed to the muscle. As in the experimental case, the hip and knee angle changes caused by the perturbation at the point of peak knee flexion during swing were recorded.
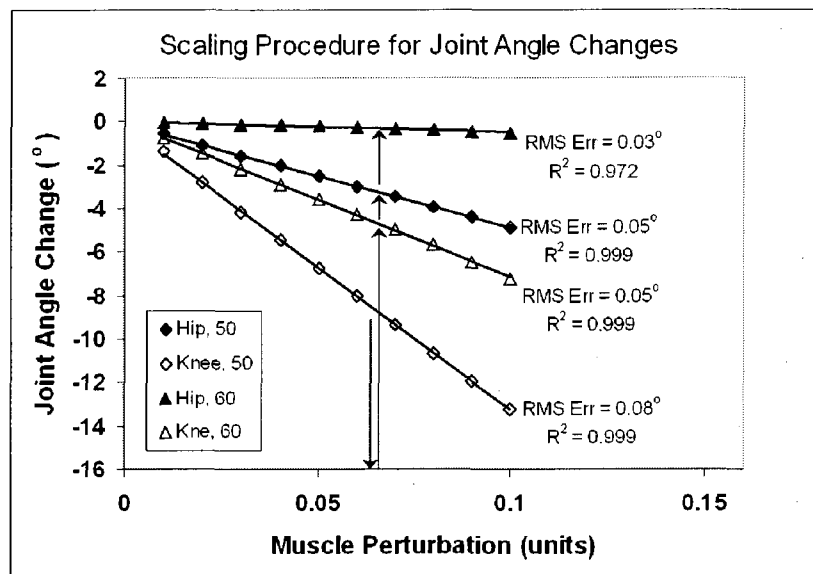
Fig. 4.5: Scaling procedure for determining the average value of the simulated joint angle changes.

The behavior of the simulated hip and knee joint angle changes with perturbation size was determined by running simulations where the perturbation size was varied in increments of 0.01 units within the range 0.01 to 0.10. The procedure was repeated twice (50% or 60% GC) generating four relationships. Each of these relationships was fitted with a line going through the origin (i.e., no joint angle change at 0 perturbation) and the root-mean-square (RMS) error of the fitted lines were noted. The typical subject above shows RMS errors less than $0.1°$ in all four relationships. On a subject-specific basis, the knee angle change for perturbation at 50% GC is matched to the experimental average for that condition. Then, the size of the perturbation that would have caused such a change is read off the x-axis. This value is then used to scale the simulation average of the hip angle at 50%GC as well as the hip and knee angles at 60%GC. For illustration, let the experimental hip angle change for stimulation at 50% GC be $-8.5°$. This value implies a perturbation size of 0.065 units. In turn, the predicted hip angle change at this condition is $-3.1°$, and the predicted knee and hip angle changes for perturbation at 60%GC are $-4.6°$ and $-0.1°$.

Because the actual level of muscle excitation occurring in the experiment is difficult to determine, a scaling procedure was developed whereby the average knee angle change in the simulation was set equal to the average knee angle change in the experiment for the 50%

GC stimulation condition. Thereafter, the simulation results for the hip perturbed at 50% GC, and for the hip and knee perturbed at 60% GC, were scaled using linear equations derived from a study of induced joint angle changes with perturbation size (Fig. 4.5).

4.3 Results

RF stimulation at 50% GC induced a significant decrease (average change of -1.0 to -14.8°) in peak knee flexion during swing in all seven subjects (Fig. 4.6). This same stimulus simultaneously acted to diminish hip flexion in four of the subjects tested (average change of -1.9° to -7.6°). Simulations of these subjects' gait patterns predicted a reduction in knee flexion in all subjects, and a reduction in hip flexion in 6 of the 7 subjects tested, with the scaled magnitude of hip angle changes comparable to that observed experimentally (Fig. 4.6).
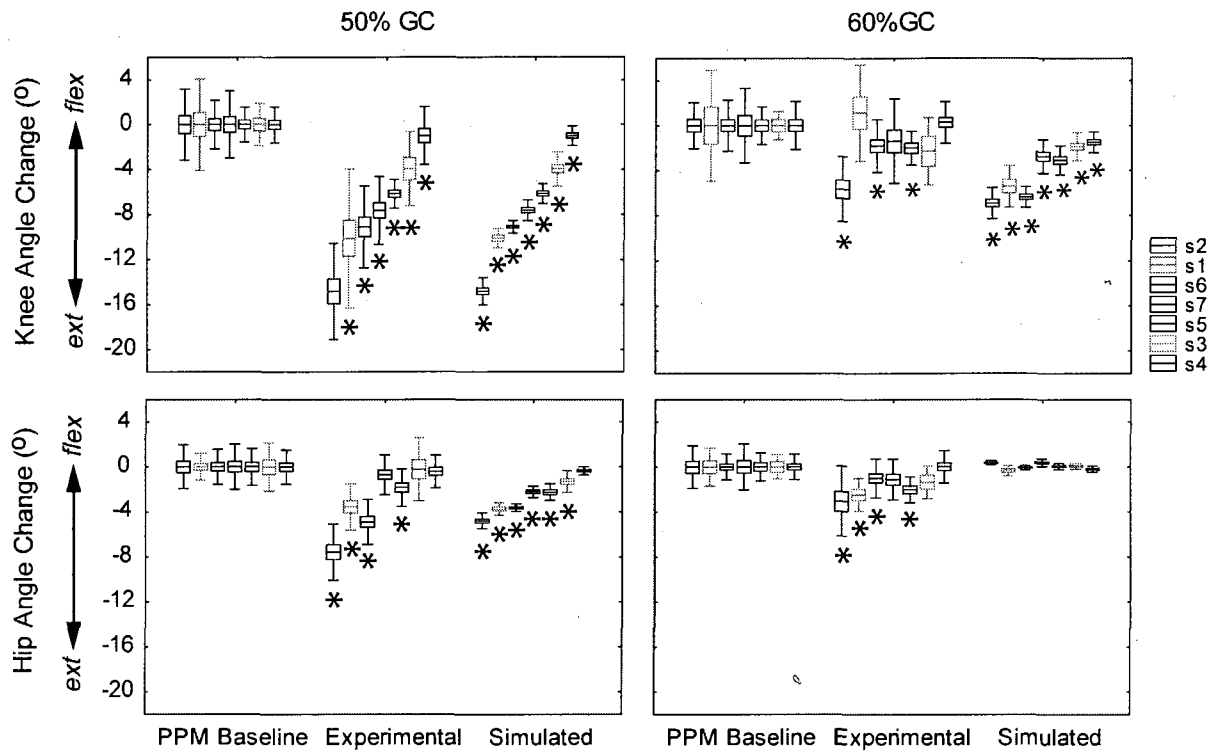
Fig. 4.6:   Hip and Knee Joint Angle Change Results

Joint angle changes for the experimental and simulated results (right two groups) in reference to baseline experimental values obtained via the periodic prediction model (left group).   Subjects have been ranked in all four plots by the order of decreasing absolute knee angle change in the 50% GC stimulation case (top left plot). Baseline and experimental values have been adjusted by the magnitude of systematic experimental errors so that all baseline values are centered at zero.   Simulated knee angle change averages for each subject have been matched to the experimental averages in the 50% GC stimulation condition.   Thereafter, the simulation averages for the remaining conditions have been scaled on a subject-specific basis using the equations derived from the musculoskeletal model (Fig. 4.5).   Central line = mean, box = standard error, whisker = standard deviation.   * = significant at p < 0.05.

Trial-to-trial variability in the model-predicted changes in hip and knee angles were significantly lower for all subjects than the variability measured experimentally in either the preceding baseline stride or the stimulated stride (Fig. 4.6, Table 4.1).   The baseline stride and the stimulated stride had similar variability.

Table 4.1: F-ratios of the variances among baseline, experimental (Exp.) and simulated (Sim.) joint angle changes.

	Subject	Stimulation at 50%GC			Stimulation at 60%GC		
		Exp. vs Baseline	Sim. vs Baseline	Sim. vs Exp.	Exp. vs Baseline	Sim. vs Baseline	Sim. vs Exp.
Knee	2	1.9	6.9 *	12.8 *	1.9	2.2	4.3 *
	1	2.3	22.4 *	51.0 *	1.3	7.1 *	5.3
	6	2.8 *	14.9 *	42.2 *	1.1	5.9 *	6.4 *
	7	1.0	10.6 *	10.9 *	1.3	4.8 *	6.2 *
	5	1.5	3.1 *	2.1	1.3	1.7	1.4
	3	3.1	1.5	4.7 *	5.7	1.0	5.7 *
	4	2.6	3.3 *	8.7 *	1.3	5.3 *	3.9
Hip	2	1.7	8.0 *	13.1 *	2.7	>100 *	>100 *
	1	3.2 *	4.4 *	13.7 *	1.4	13.7 *	10.1 *
	6	1.7	21.3 *	35.2 *	2.3	36.8 *	84.1 *
	7	1.3	15.0 *	11.9 *	1.2	35.2 *	28.4 *
	5	1.1	4.7 *	5.0 *	1.1	21.7 *	19.2 *
	3	1.7	4.9 *	8.4 *	1.7	17.8 *	30.7 *
	4	1.1	18.3 *	16.5 *	1.6	19.6 *	31.7 *

F-ratio = $\dfrac{\sigma_1^2}{\sigma_2^2}$ where $\sigma_1 > \sigma_2$ are the standard deviations of the samples to be compared.

* Significant at $p < 0.05$.

RF stimulation at 60% GC induced a decrease in peak knee flexion during swing in 3 of the 7 subjects tested, with this change being much lower than was observed with the 50% GC stimulus (Fig. 4.6). The 60% GC stimulus also diminished hip flexion in the same four subjects who showed a change in hip flexion in the 50% GC case. The gait simulations correctly predicted that the 60% GC stimulation would have a lesser effect on knee flexion in

swing, but also incorrectly predicted no effect of the 60% GC stimulus on hip flexion.

Trial-to-trial variability in the model-predicted changes in hip and knee angles were again

significantly lower for all subjects than the variability measured experimentally in either the

preceding baseline stride or the stimulated stride (Table 4.1).

RF 50% GC Condition

RF 60% GC Condition
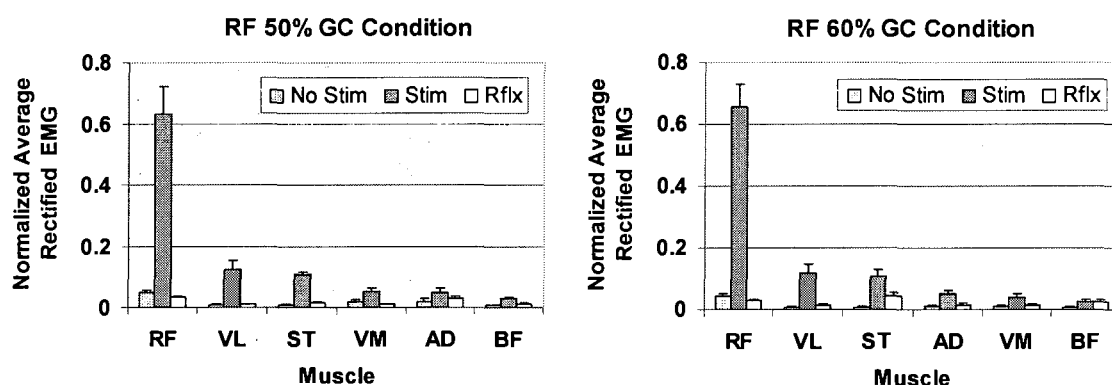
Fig. 4.7:   Comparison of muscle rectified EMG activity in non-stimulated strides preceding each stimulus (No Stim), stimulated strides (Stim), and in a potential reflex activity window following each stimulated stride. The window of observation is 0-150 ms for the stimulated and non stimulated stride categories, and 150-300 ms for the reflex category, where 0 ms marks the onset of the stimulus.   The results above represent averages across subjects.   For each subject and category, the rectified EMG activity of each muscle was normalized by the total rectified EMG of all muscles such that the sum of the normalized values for all muscles was 1. The data for the non stimulated stride and reflex categories were then normalized once more, this time by the ratio of the total rectified EMG of the stimulated strides to the corresponding total for the category of interest.   In this manner, the relative EMG magnitudes between the three categories was preserved.

EMG measurements confirmed that the stimulus primarily induced activity in the RF,

with a large majority of the net EMG activity being measured in that muscle during a 150 ms

period following the stimulus (Fig. 4.7, middle bars).   The normal activity of any muscle

during an equivalent 150 ms period in the non-stimulated strides (left bars) was less than 10%

of the EMG value measured from RF in the stimulated strides. The average activity of any

muscle in the 150-300 ms period following the stimulus, where we might expect reflexes to

occur, was less than 8% of the RF EMG average during the stimulated stride.

4.4   Discussion

This study shows that activation of the RF prior to toe-off can substantially diminish

knee flexion during swing. The result at the knee agrees with dynamic gait models that have

shown that knee flexion velocity at toe-off is a major determinant of knee flexion during

swing [9, 10, 46]. Thus, early onset of the RF during double support likely reduces knee

flexion velocity. Our results agree with those of a recent study where the RF of CP patients

was treated with botulinum toxin injection [80]. In that study, the inactivity of the RF

induced by the toxin caused the knee to flex more than when the muscle was over-active, and

the effect was larger in patients whose RF over-activity was during pre-swing than in patients

whose RF over-activity was during early swing.

Stimulation of the RF also induced extension at the hip in a majority of the subjects,

which is opposite to the hip flexor moment generated by this muscle. Such an effect reflects inter-segmental dynamics, in which biarticular muscles can induce non-intuitive motion at one joint via their action at a neighboring joint [48]. In this study, the induced knee extension was roughly 2.7 times larger than the hip extension if the stimulus occurred during pre-swing, which is comparable to the average changes predicted by the gait model (Fig. 4.6). However, our gait simulations were unable to predict induced hip motion at the 60% GC conditions. Our gait simulations did reflect individual walking patterns and also accounted for variations in stimulus magnitude, as determined by scaling to motion induced at the knee. Variability in muscle moment arms are known to have a large effect on the relative motion induced by RF at the hip and knee [26] and likely contributed to discrepancy seen with experimental data. Given that pathological subjects can exhibit tremendous differences in muscle moment arms due to abnormal bone geometry, it would seem judicious to proceed with caution when using generic models to evaluate treatment in patients with stiff knee gait.

If the RF is indeed a hip and knee extensor at the point of its normal activity during walking (around toe-off), as our experiment indicates, it is then possible that RF release or transfer in stiff-knee gait cases may result in the conversion of the RF from a hip extensor into a hip flexor. So, even though the description of the RF as a hip flexor would be inadequate in

healthy subjects, it would likely be correct in persons where the RF has been distally released, because the knee extensor moment, which induces hip extension acceleration via dynamic coupling, would no longer exist. Therefore, releasing the RF would likely have two effects on the subject: one from eliminating the knee extensor moment (which should relieve the stiff-knee symptom) and another from allowing the RF to act as a hip flexor.

The variability between the baseline and experimental data was similar (F-ratios not significant). Hence, significant differences between the experimental data and the baseline are mostly due to displacements of the average value (i.e., a true extension effect). Secondly, the distributions in the simulated data are often much tighter and vary less across subjects than those in the experimental and baseline data (Fig. 4.6). This result suggests that differences in overall size or segment inertias among subjects is only a small contribution to the overall variance in the data. Rather, the increased variance seems to arise from stride-to-stride variability in the subject's walking pattern. This variability influences the ability of the periodic prediction model to accurately predict the behavior of the next stride. The error in the predictions accounts for the observed variance. We also note that some subjects (e.g., subject 5, RF 50%GC condition) can achieve tight distributions that are of the order predicted by the simulation, which suggests that some persons walk with more

consistent strides than others. It is possible that the amount of stride-to-stride variability was influenced by having an indwelling electrode inserted in the thigh.

The normalized values of the rectified EMG measurements were much larger (>10X) for the RF during stimulated strides than during non-stimulated strides whether the stimulus was delivered before (50% GC) or after (60% GC) toe-off (Fig. 4.7). Similarly, the EMG recordings of the RF during the 1-150 ms following the stimulus were much larger than the EMG recordings of all muscles (including the RF) in the 150-300 ms window. This 150-300 ms period is considered a period where reflex activity may ensue. EMG activity within the window 90-150 ms following stimulus onset was not considered in the reflex category because that period is contaminated with the stimulus response signal, which is often still decaying (Fig. 4.2). We conclude that the RF is receiving most of the stimulus and is likely responsible for most of the active force driving the motion. We acknowledge, though, the potential for forces to be developing in other muscles due to stretch [81].

4.5   Conclusion

A new methodology for the evaluation of dynamic muscle function has been

introduced, whereby a muscle can be electrically stimulated for a short period of time and its effects on joint angles measured. We used this methodology to assess the effect of electrically stimulating the rectus femoris during pre-swing or early swing on the peak knee flexion during swing. We showed that stimulating the RF during pre-swing induces significant hip and knee extension and that stimulating this muscle during early swing induces a smaller effect, still into extension. Similarly perturbed forward dynamic simulations predicted these overall trends but were not highly accurate predicting subject-specific values. They also failed to predict a small amount of hip motion that was experimentally observed in several subjecs. We conclude that early onset of RF activity has a greater potential than increased activity of this muscle during swing to contribute to stiff-knee gait, and that clinical treatments should consider the counter-intuitive function that the RF has in extending the hip.

Chapter 5

Measurement and Simulation of Dynamic Hamstring Muscle Function during Normal Walking

Biarticular muscles are often implicated in gait abnormalities. For example, tightness and/or over-activation of the biarticular hamstrings are considered contributors to crouch gait, which is characterized by excessive knee flexion during stance, often accompanied by hip flexion, adduction and internal rotation [82, 83]. In children, crouch gait is often treated aggressively to circumvent long-term joint degeneration and disability. However, treatment outcomes remain inconsistent [84]. This inconsistency may in part reflect that the hamstrings on some of these children are not actually short [85], such that other factors (e.g., activation levels, muscle forces and multi-joint dynamics) may be contributing to their crouched gait.

Various groups of investigators have used dynamic simulations to understand the contributions of hamstrings to limb motion in both normal and pathological conditions [17, 86]. One such group has predicted that the hamstring muscles act to induce hip extension and nearly no motion at the knee, at the point when these muscles are normally active (terminal swing) [84]. Another team has suggested that the hamstrings may actually induce knee extension during stance, particularly in crouched postures [69]. Such non-intuitive function can arise from dynamic coupling [48], in which the hip extensor moment generated by the hamstrings induces the knee extension motion.

While providing important insights, there are a number of assumptions and limitations inherent in gait simulations which make it challenging to translate their results to clinical treatment. First of all, most models rely on generic descriptions of musculoskeletal geometry which do not account for the subject-specific variations in muscle moment arms that are known to affect function [26, 48]. Secondly, muscle induced accelerations, which are often computed from gait simulations, are known to be sensitive to the number of degrees of freedom included in a musculoskeletal model [19]. Finally, a muscle's induced acceleration on a body segment represents instantaneous movement that the muscle would induce in isolation. However, in clinical gait analysis, clinicians typically observe

movement at the position level which is the integrated net accelerations in the system. Hence, the induced positions at the joint level will necessarily occur sometime after excitations are observed, and will also reflect both mechanical and neural interactions within the entire neuromusculoskeletal system. As an example of the importance of this issue, recent observations strongly suggest that stiff-knee (limited knee flexion in swing) gait is likely dependent on abnormal muscle activities in stance [16]. As another example, crouch gait has been traditionally attributed to prolonged hamstring activity in stance [83]. However, it could analogously be the case that hamstring activity during swing induces abnormal motion that is later observed in stance.

Recently, investigators have initiated the use of electrical stimulation perturbations to perform *in vivo* measurements of the influence of muscles on limb movements [26, 69, 70, 87]. For example, Stewart et al. [69] found that the biarticular hamstrings could extend the knee in healthy subjects if they were standing in a crouched posture but not if they were standing upright. Our group has established an electrical stimulation protocol for the direct measurement of dynamic muscle function during walking (see Chapter 4). The purpose of this study was to use this protocol to analyze dynamic medial hamstring function at the terminal swing–to-early stance transition in normal gait. We hypothesized that hamstring

activity during terminal swing would act to extend the hip and flex the knee during stance, and that the magnitude of the induced motion would be reduced if the activity happened after heel contact.

5.1 Methods

5.1.1 Experimental Methodology

Seven healthy young adults (age = 30.7 ± 6.3 yr, mass = 71.2 ± 10.0 kg, height = 1.75 $\pm$ 0.06 m) participated in this study, which was approved by the University of Wisconsin's Health Sciences Internal Review Board. The protocol requested that subjects perform 90 s walking trials on a split-belt instrumented treadmill (Bertec Corp., Columbus, OH) while their right semitendinosus was briefly stimulated during terminal swing or early stance on randomly-selected strides (Fig. 5.1).

5.1.2 Electrical stimulation synchronized to the gait cycle

A dual-channel, current-controlled stimulator (Grass S88, Astro-Med, Inc., West Warwick, RI) was used to stimulate the muscle. We first located the motor point of the ST by

moving surface stimulating electrodes over the skin until a maximum twitch response was observed. The optimal electrode positions were then cleaned with alcohol and primed with conductive gel prior to the placement of new, self-adhering surface electrodes. Our surface electrodes were cut down to a size of approximately 1.25"x 1.5" to avoid stimulus spill-over to other muscles. Ninety ms current pulse trains (four 300 µs pulses at 33 Hz) were delivered to the ST at select times on random gait cycles. The stimulating current (≤ 50 mA) was set for each subject independently at a level that elicited hip and/or knee motion but was easily tolerated. Stimulation timing was controlled by using a custom LabView (National Instruments, Austin, TX) program to monitor vertical ground reactions under each foot in real time. The forces were then used to detect heel strikes, from which the stride duration was calculated. Based on the average period of the last 3 strides, the controller then triggered the muscle stimulator at either 90% (terminal swing) or 0% (early stance) of the gait cycle. A minimum of five non-stimulated strides followed, with the subsequent stimulus randomly introduced in one of the following five strides.

a.   b.   c.
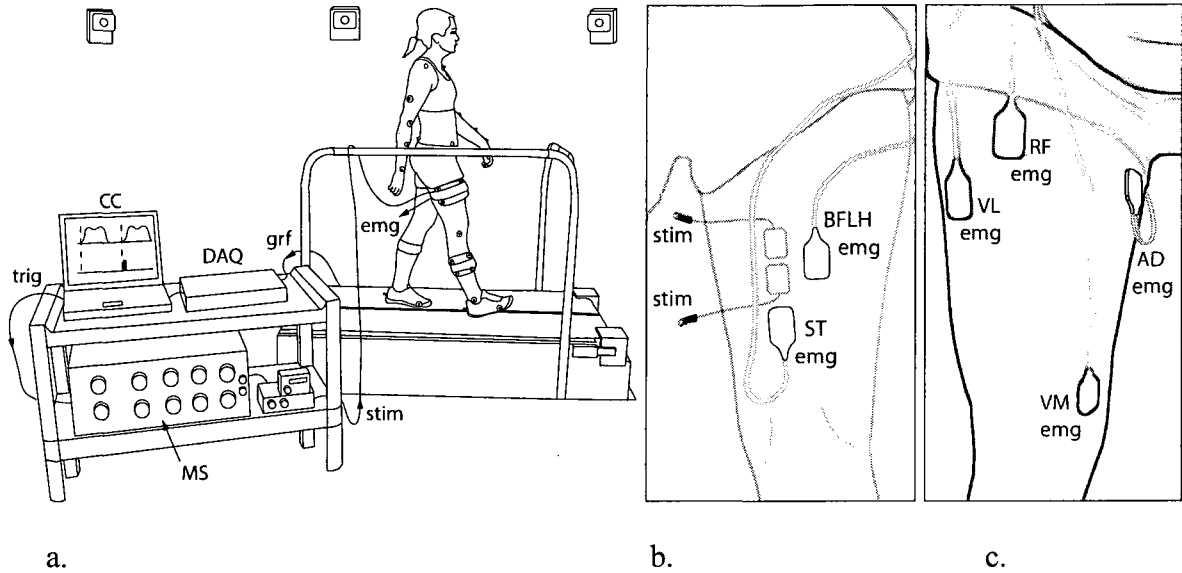
Fig. 5.1: Experimental Setup.

(a) A subject is walking on a split-belt force-plate instrumented treadmill while a computer controller monitors ground reaction forces.   Based on the frequency of heel strikes, the controller estimates the stride period in real time and stimulates the muscle at a pre-specified percentage (90%, 0%) of the gait cycle.   The stimulation causes the trajectories of the markers to change in the current stride, and these changes are recorded by a high speed motion capture system.   Inverse kinematics is then used to determine the experimental joint angles.   (b) The ST was stimulated using surface electrodes, and EMG was recorded from the rectus femoris, vastus medialis, vastus lateralis, semitendinosus, biceps femoris long head, and adductor muscle group to assess stimulus spillover and reflex activity.   CC = computer controller, DAQ = data acquisition unit, MS = muscle stimulator, grf = ground reaction force signals, trig = trigger signal, stim = stimulation train signal, emg = EMG signals to motion capture software, BFLH = biceps femoris long head, ST = semitendinosus, RF = rectus femoris, VL = vastus lateralis, VM = vastus medialis, AD = hip adductors.

5.1.3 Kinematics

Three-dimensional whole body kinematics were recorded at 100 Hz using an 8-camera motion capture system (Motion Analysis, Santa Rosa, CA) to track 44 reflective markers (Fig. 5.1.a).   Twenty-five markers were placed over anatomical bony landmarks and

the other tracking markers were attached to plates that were strapped tightly to lower limb segments. All kinematic data was low-pass filtered at 6 Hz. Joint angles were computed using a whole body model that included 23 segments and 21 lower extremity degrees of freedom (d.o.f.) to represent the low back, hip, knee and ankle joints [72]. The pelvis was the base segment with 6 d.o.f. Each lower limb included a 3 d.o.f. ball-and-socket representation of the hip, a 2 d.o.f. ankle with non-intersecting talocrural and subtalar joints [5], and a 1 d.o.f. knee where translations and non-sagittal rotations were functions of knee flexion [73].

Segment lengths in the model were first scaled to each subject using anatomical marker positions measured in a standing upright trial. The hip joint center in the pelvic reference frame was then calibrated using a functional joint center identification routine [56]. At each frame of a motion trial, we then used a global optimization inverse kinematics routine to compute pelvic position and joint angles that minimize the discrepancy between measured marker positions and corresponding markers fixed to the body segments [74].

5.1.4 Muscle Activity

Pre-amplified, single differential EMG electrodes (DE-2.1, DelSys Inc., Boston,

MA) were placed on the rectus femoris, vastus lateralis, vastus medialis, semitendinosus,

biceps femoris and adductor muscle group of the right limb (Fig. 5.1.b).
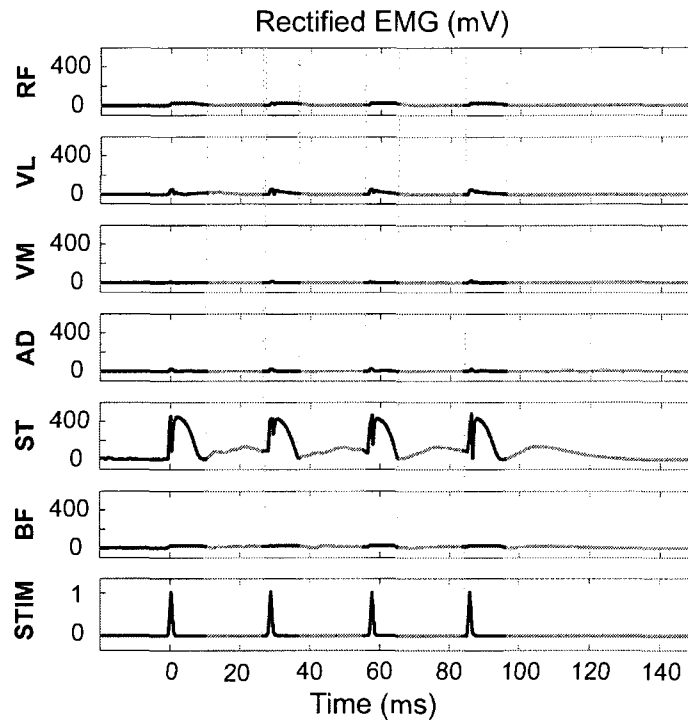
Fig. 5.2: Stimulation current (normalized to 1) and ensuing muscle EMG recordings in μV.

The shaded regions correspond to the regions where the rectified EMG was measured. For each stimulated stride, the central low point in the M-curve following each of the first three pulses was identified and a window created between this point and a point 1 ms from the next stimulus pulse. The window for the fourth (and last) stimulus pulse ended at 150 ms to ensure that the stimulus had decayed to zero before looking at potential reflex activity in the subsequent 150 ms window. Abbreviations: STIM = stimulation pulses, BF= biceps femoris, ST = semitendinosus, AD = adductors, VM = vastus medialis, VL = vastus lateralis, RF = rectus femoris.

These EMG activities, the ground reaction forces from the treadmill and the

stimulator's trigger signal were sampled synchronously at 2000 Hz. The EMG recordings

were later rectified and used to evaluate stimulus spill-over (within 150 ms following

stimulus onset) and potential reflex activity (150-300 ms after stimulus onset) occurring in

non-stimulated leg muscles as a consequence of the electrical stimulation (Fig. 5.2).

5.1.5 Joint Angle Change Calculations

To determine the joint angles induced by the stimulus at the hip and knee, we first

plotted the hip and knee angle curves for each stimulated stride and the stride preceding it

(Fig. 5.3). We looked for the point of minimum knee flexion that occurs just prior to initial

contact in both the stimulated and non-stimulated strides. Secondly, we found the point of

peak knee flexion during stance in the stimulated stride and determined the time lapse

between the minimum and maximum knee flexion points ($t_{min-max}$). We then found a

corresponding point of expected peak knee flexion in the non-stimulated stride as the time

point of minimum knee flexion plus $t_{min-max}$. This point estimated, but did not overlap, the

point of peak knee flexion in the non-stimulated stride, because the stimulus induces a change

in the time to reach peak knee flexion. However, keeping the time lapse constant across

conditions (90% or 0% GC stimulation) and joints (hip, knee) allowed us to ask the question:

how did the stimulus affect the joint angles differentially between the conditions and between

the joints?
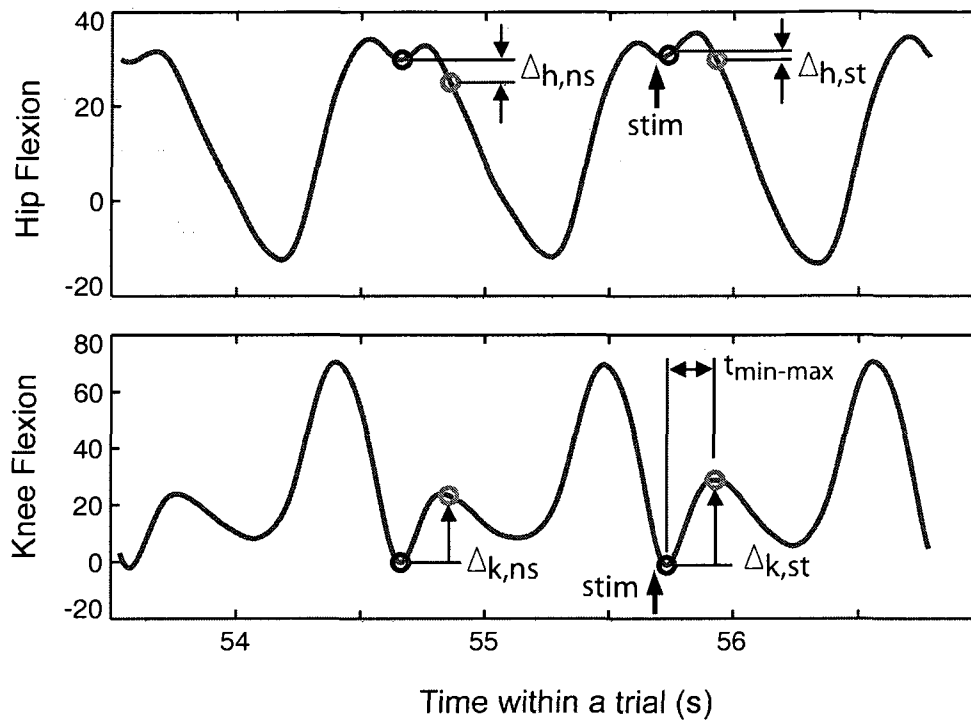
Fig. 5.3. Computation of hip and knee flexion angle changes shown for ST stimulation at 90% of the gait cycle. The point of minimum (dark blue) and maximum (light green) knee flexion during the terminal swing to early stance transition were identified in the stimulated stride (far right). The time lapse between these two points ($t_{min-max}$) was stored. The point of minimum knee flexion in the previous, non-stimulated stride was identified and used as an anchor point. The corresponding maximum point was determined as the point of minimum knee flexion plus the difference $t_{min-max}$. These time points were used as the limits for computing both the knee and hip angle changes of the stimulated and non-stimulated stride. Note that the maximum point in the non-stimulated stride is only an approximation of the true maximum; however, keeping the time difference constant between the stimulated and non-stimulated stride, and between the hip and knee, allowed for fair joint angle change comparisons to be made. Δ = deviation, h = hip, k = knee, ns = non-stimulated stride, st = stimulated stride.

The difference between the actual and predicted hip and knee angles were evaluated at the point of predicted peak knee flexion during swing in the stimulated stride. Similarly, the difference between the actual and predicted hip and knee angles was evaluated at a point

one period behind. The difference between these two changes was considered to be the effect of the stimulus. The mean effects of the stimulated and corresponding non-stimulated strides of each trial were compared using t-tests to determine if the differences were statistically significant ($\alpha= 0.05$). The experimental effects were also qualitatively compared to the predictions of forward dynamic simulations similarly perturbed.
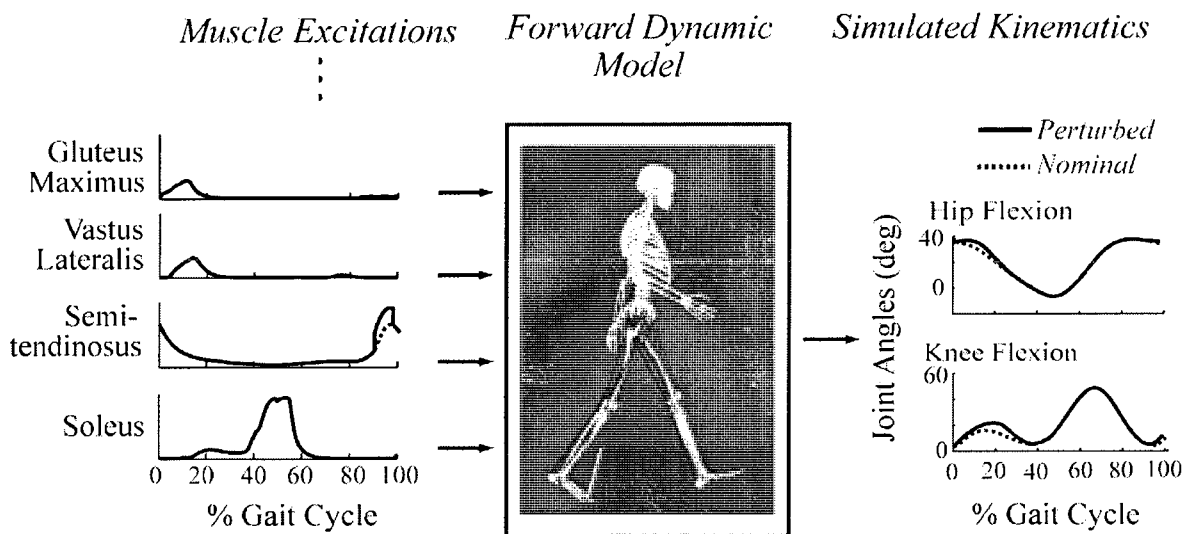
Fig. 5.4: Method of perturbing forward dynamic simulations.

A 100 ms, 0.1 unit increase in the semitendinosus' nominal excitation was introduced at 90% or 0% of the gait cycle. The altered RF excitation and the nominal excitation of the other muscles were applied to the model to generate perturbed forward dynamic simulations. The perturbation-induced changes in hip and knee flexion were recorded.

5.1.6 Subject-specific forward dynamic simulations of gait

Scaled whole body models were also used to develop simulations of subject-specific walking dynamics. We included 92 musculotendon actuators that represented the major muscles acting about the low back, hip, knee and ankle joints [5]. The input to each muscle was an excitation that could vary between 0 and 1. Excitation-to-activation dynamics was represented by a bi-linear differential equation with activation and deactivation time constants of 10 and 40 ms, respectively [76]. A Hill-type musculotendon model was used to describe contraction dynamics [77]. For each subject, we generated simulations of the normal gait stride that preceded a stimulation pulse train. In these simulations, computed muscle control was used to determine a set of muscle excitations that drove the model to closely track measured lower extremity kinematics, while upper extremity kinematics were prescribed to track measured values. This approach has previously been shown to produce simulations of lower extremity joint angles that are within ~1° of measurements [7]. Excitations were determined that minimized the weighted sum of squared muscle activations [78], which is known to provide reasonable estimates of coordination patterns seen in normal gait [72].

After generating a nominal simulation, we then perturbed the ST excitation patterns

at either 90% (terminal swing) or 0% (early stance) of the gait cycle (Fig. 5.4). This was

done by increasing the excitation level of the ST by 0.1 unit (1 corresponds to maximum

excitation drive) for a 100 ms period. Changes in the interactions between the stance-limb

foot and the ground were characterized by a set of rotational and translational spring-damper

units [79]. Hence, the ground reaction forces and moments were allowed to change in

response to the perturbations in force, and the effects of these changes were implicitly

included in the actions attributed to the muscle. As in the experimental case, the hip and

knee angle changes caused by the perturbation at the point of perturbed peak knee flexion

during stance were recorded.

Because the actual level of muscle excitation occurring in the experiment is difficult

to determine, a scaling procedure was developed whereby the average knee angle change in

the simulation was set equal to the average knee angle change in the experiment for the 90%

GC stimulation condition. Thereafter, the simulation results for the hip at 90% GC

stimulation, and for the hip and knee at 0% GC stimulation were scaled using linear equations

derived from a study of induced joint angle changes with perturbation size (Fig. 5.5).
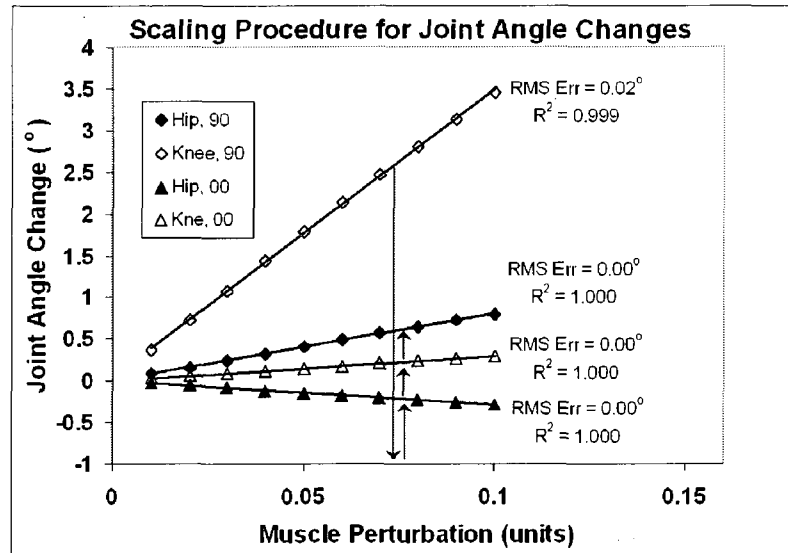
Fig. 5.5: Scaling procedure for determining the average value of the simulated hip and knee angle changes. The behavior of the simulated joint angle changes with perturbation size was determined by running simulations where the perturbation size was varied in increments of 0.01 units within the range 0.01 to 0.1 and recording the values for the hip and knee joint angles changes. The procedure was repeated twice (stimulations at 90% or 0% GC) generating four relationships. Each of these relationships was fitted with a line going through the origin (i.e., no joint angle change at 0 perturbation) and the value of the root-mean-square (RMS) errors was noted. (The subject above shows RMS errors less than $0.02°$ in all four relationships.) On a subject-specific basis, the knee angle change for stimulation at 90% GC is matched to the experimental average for that condition. Then, the size of the perturbation that would have caused such a change is read off the x-axis. This value is then used to determine the expected simulation average of the hip angle at 90%GC as well as the hip and knee angles at 0%GC. For illustration, let the experimental value in the figure above be $2.5°$. This value implies a perturbation size of 0.07 units. In turn, the predicted hip angle at this condition is $0.6°$, and the predicted knee and hip angles for perturbation at 0%GC are $0.2°$ and $-0.2°$.

5.2 Results

Electrical stimulation of the ST at 90% GC induced a significant increase (average change of $2.1°$ to $6.8°$) in peak knee flexion during stance in five of seven subjects (Fig. 5.6).

This same stimulus simultaneously extended the hip in 3 subjects (average of -1.4° to -1.7°), flexed it in two (0.9° to 1.1°), and had no effect in another two (0.2° to 0.6°). Interestingly, the three subjects who showed the smallest changes in knee flexion were the same subjects who exhibited hip extension, while the subjects who showed the greatest amounts of knee flexion exhibited the largest increases in hip flexion.

For dynamic simulations perturbed at 90% GC, the variability in the simulated knee angle changes was generally much smaller than in the experimental case (Fig. 5.6). Hence, the comparison of simulated knee angle changes with the baseline reached significance for all of the five subjects that had displayed significance experimentally. However, even with smaller variability, the model predictions were not significantly different from the baseline data for the other two subjects. This result suggests that the experimentally observed changes for these two subjects were too small to be considered flexions even in the absence of experimental errors. At the hip, the model predicted a tendency towards flexion, though this effect was small and reached significance in only two of the subjects (Fig. 5.6). Experimentally, we observed a similar tendency toward flexion in four subjects (significant in two of them). However, in three of the five cases where the simulation predicted no change, the experiment yielded significant hip extension.
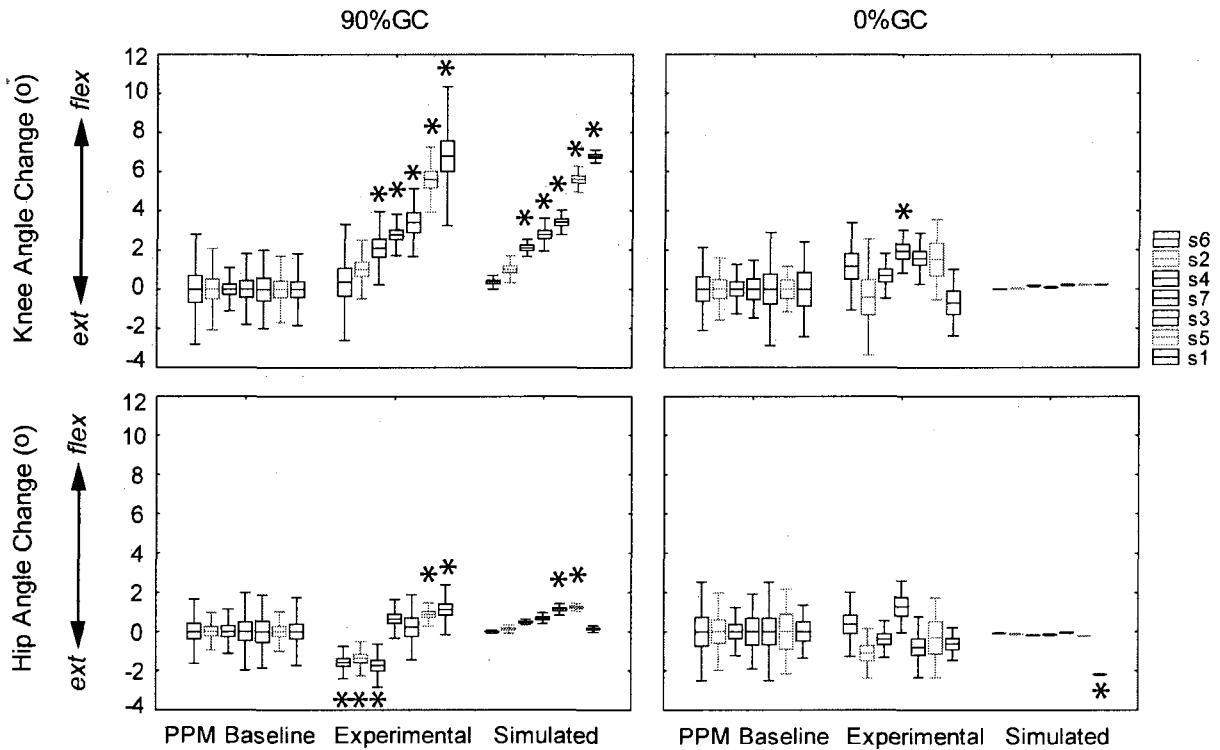
Fig. 5.6: Joint angle changes for the experimental (stimulated strides) and simulated (perturbed strides) groups in reference to baseline (non stimulated strides).

Subjects have been ranked in all conditions by order of increasing knee angle change in the 90% GC stimulation case. Non-stimulated strides and stimulated strides have been adjusted by the magnitude of systematic experimental errors so that all baseline values are centered at zero. Simulated knee averages for each subject have been matched to the experimental averages in the 90% GC stimulation condition. Thereafter, the simulation averages for the remaining conditions have been scaled on a subject-specific basis using the equations derived from the musculoskeletal model (Fig. 5.5). Central line = mean, box = standard error, whisker = standard deviation. * = significant at $p < 0.05$.

ST stimulation at 0% GC induced an increase in peak knee flexion during swing in only 1 of the 7 subjects tested, and no changes in hip angles. The gait simulations correctly predicted that the 0% GC stimulation would have a lesser effect on peak knee flexion and hip joint angles.

Trial-to-trial variability in the model-predicted changes in joint angles were significantly lower for all subjects than the joint angle changes measured experimentally in either the baseline (non-stimulated) stride or the stimulated stride (Table 1). This effect was seen whether the stimulus was introduced at 90% or 0%GC. On the other hand, the baseline stride and the stimulated stride had similar variability.

Table 5.1: F-ratios of the variances among baseline, experimental (Exp.) and simulated (Sim.) joint angle changes.

	Subject	90%GC			0%GC		
		Exp. vs Baseline	Sim. vs Baseline	Sim. vs Exp.	Exp. vs Baseline	Sim. vs Baseline	Sim. vs Exp.
Knee	6	1.1	64.6 *	71.9 *	1.1	>100 *	>100 *
	2	1.9	9.3 *	4.7 *	3.4 *	>100 *	>100 *
	4	2.9 *	6.3 *	18.2 *	1.2	>100 *	>100 *
	7	2.9 *	4.5 *	1.5	1.8	>100 *	>100 *
	3	1.3	10.4 *	7.9 *	4.9 *	>100 *	>100 *
	5	1.04	6.7 *	6.4 *	3.2	>100 *	>100 *
	1	3.7 *	31.9 *	>100 *	2.0	>100 *	>100 *
Hip	6	3.9 *	374.1*	96.8 *	2.4	>100 *	>100 *
	2	1.2	19.9 *	16.6 *	2.4	>100 *	>100 *
	4	1.0	61.6 *	59.2 *	1.7	>100 *	>100 *
	7	4.0 *	49.4 *	12.4 *	2.1	>100 *	>100 *
	3	1.3	40.5 *	31.9 *	2.6	>100 *	>100 *
	5	2.8 *	23.5 *	8.1 *	1.1	>100 *	>100 *
	1	1.9	>100 *	59.9 *	2.7	>100 *	>100 *

F-ratio = $\dfrac{\sigma_1^2}{\sigma_2^2}$ where $\sigma_1 > \sigma_2$ are the standard deviations of the samples to be compared.

* Significant at $p < 0.05$.

EMG measurements confirmed that the stimulus primarily induced activity in the ST,

with a large majority of the total EMG activity being measured in that muscle, during the 150

ms period following the stimulus (Fig. 5.7, middle bars).

ST 90% GC Condition　　　　　　　　　　**ST 0% GC Condition**
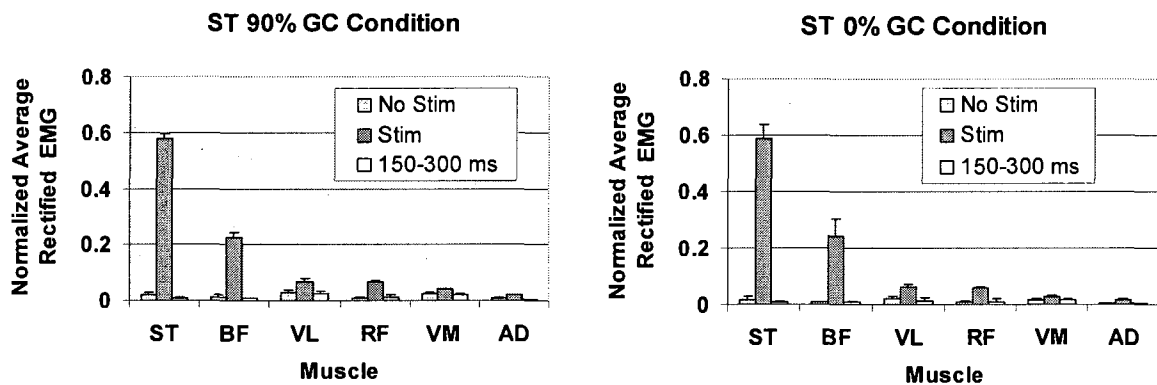
Fig. 5.7:　Comparison of muscle rectified EMG activity in non-stimulated strides preceding each stimulus (No Stim), stimulated strides (Stim), and in a potential reflex activity window following each stimulated stride. The window of observation is 0-150 ms for the stimulated and no stimulation categories, and 150-300 ms for the reflex category, where 0 ms marks the onset of the stimulus. The results above represent averages across subjects. For each subject and category, the rectified EMG activity of each muscle was normalized by the sum of all muscles' rectified EMG such that the sum of the normalized values for all muscles was 1. The data for the no stimulation and reflex categories was then normalized once more, this time by the ratio of the rectified EMG sum of the stimulated strides to the corresponding sum for the category of interest. In this manner, the relative EMG magnitudes between the stimulated strides and the other two categories were preserved.

The normal activity of any muscle during an equivalent 150 ms period in the non-stimulated

strides (left bars) was less than 10% of the EMG value measured from ST in the stimulated

strides. The average activity of any muscle in the 150-300 ms period following the stimulus,

where we might expect reflexes to occur, was less than 8% of the ST average EMG during the stimulated stride.

5.3 Discussion

We have shown that the timing of hamstring activity will substantially affect the amount of knee flexion observed in stance. The hamstrings are normally active from about 15% GC prior to heel contact (HC) up to about 5% GC after HC, except for semitendinosus, which is active from about 10% before HC up to about 15% after HC [53]. Our results suggest that hamstring activity prior to HC has a greater potential to induce a more flexed knee during stance than hamstring activity occurring after HC. Such delays between stimulation and induced motion are likely attributable to activation, contraction and skeletal dynamic processes. Indeed, the inclusion of these factors in our model resulted in predicted induced movement magnitudes that generally agreed with our experiments.

We observed relatively small effects of 90% GC hamstring stimulation on hip motion, with three subjects exhibiting a small increase in hip extension and two subjects exhibiting a small increase in hip flexion. Prior studies suggest that hamstring forces may

counter-intuitively induce a hip flexion acceleration when active during swing [10], but then induce a hip extension acceleration during stance [88]. Due to activation and contraction dynamics, the 90% GC stimulation would result in a perturbation to hamstring force that overlaps both swing and stance phases. Thus, it is feasible that the induced motion observed in a subject could be a combination of the muscle's varying function through this region and, as a result, may exhibit a different net motion depending on the exact timing and magnitude of the stimulus. Other factors that may contribute to inter-subject variability are differences in the relative moment arms of the hamstrings at the hip and knee, which would greatly affect the movement induced at a joint [48].

In addition to contributing to limb motion, the hamstrings may also play an important role in modulating the forward acceleration of the center of mass. Previous modeling studies suggest that the active hamstrings would induce forward propulsion during early stance [86, 89], even though the net acceleration of center of mass is backward. Our simulations show similar patterns, with hamstring activity during late swing being an effective way of decreasing the braking force seen in the first half of stance. It is feasible then that enhanced hamstring activity may be used functionally to, for example, compensate for diminished ankle plantar flexor contributions to forward propulsion on the opposite limb. For example,

Schmitz et al. studied muscle activation patterns in older adults and found evidence of extended hamstring activity in conjunction with reduced ankle plantar flexor activity when walking speed was increased [90]. Further analysis of our experimental ground reaction data is needed to determine whether we can detect differences in ground reactions as a function of hamstring stimulation.

A critical aspect of this study is its relevance for treating crouch gait in children with neurological disorders. Traditionally, it has been thought that the observed extended activity of the ST during stance may be responsible for crouch gait [83]. However, in our study, we have shown that increased hamstring forces starting in late swing, e.g., as a result of passive stretch of a tight muscle or enhanced activity due to spasticity, would likely contribute to a more flexed limb posture during stance. Treatment options for crouch gait can include hamstring lengthening surgery [91], hamstring transfer surgery [92] or pharmacologic treatment to reduce spasticity. Each of these treatments would have a differential effect on function. Hamstring lengthening or anti-spasticity medication should reduce both the hip and knee flexor moment generated by the hamstrings. Hence, function of the muscle may remain relatively unchanged but the magnitude of its effect would be diminished due to less force. Alternatively, hamstring transfer surgery would theoretically retain the hip extension

moment capability, while eliminating moment generation about the knee [92]. In this regard, the hamstring's hip extensor moment would likely induce hip and knee extension in late swing which could reduce crouch, but further analysis would be needed to see if it can still be used to modulate ground reactions.

There are a number of limitations of the study that should be considered in interpreting the results. First of all, we used surface electrodes for stimulation which, due to stimulus spillover, limited our ability to ensure that the stimulus went into our targeted muscle. We analyzed muscle EMG activities between stimulation pulses to assess the extent of this problem and confirmed that the largest amount of muscle activity was indeed induced in the medial hamstrings (Fig. 5.7). Induced reflex activity could also contribute to the motion observed. However, we found no significant increases in muscle activities during the time frame 150-300 ms after stimulation onset, over which we quantified the induced motion, which suggests that reflex contributions were relatively small.

For semitendinosus stimulation during terminal swing, we observed an inconsistent response, with some subjects showing low levels of hip flexion and others showing low levels of hip extension. A potential confounding factor would exist if the stimulus generated a flexion withdrawal response during early stance in some of the subjects. This would have

been best analyzed by collecting EMG on the contralateral limb for evidence of a cross extension response, something that we did not do. Two pieces of information suggest that there was not a flexion withdrawal response in our subjects. Firstly, we did not measure a reduction in ipsilateral knee extensor muscle activities (vastus lateralis and vastus medialis) during the potential reflex window in these subjects, which would have been consistent with a flexor withdrawal response. Second, the absence of significant hip and knee flexion for stimulation at 0% GC shows that there was not a flexion withdrawal response for stimulation during stance. Therefore, we would have seen a flexion withdrawal response in some subjects for the 90% GC stimulation case only if there was pain present at this condition but not in the 0% GC stimulation case. We monitored subjects' pain levels and in no case did subjects complain of differential pain dependent on test trial. In fact, subjects only reported mild discomfort (not pain) throughout the trials.

Induced motion was ascertained by computing the change in hip and knee angles, relative to the previous stride. However, simple stride-to-stride variability movement will contribute to some of the measured changes and thus introduce noise into our induced motion measurements. We took measurements over many strides and compared them statistically to overcome this variability. As a result, the measured induced joint angles exhibit

substantially larger variability across strides than the simulations.

Finally, we have measured hamstring-induced motion under one condition – normal gait at a preferred speed. Children with cerebral palsy exhibit abnormal kinematics and often slow walking patterns, both of which will affect muscle function. Thus further analysis of children exhibiting crouch gait is an important area of future research.

5.4   Conclusion

We conclude that consideration of time delays due to muscle and skeletal dynamics is critical to properly interpret how muscle activation patterns can contribute to gait patterns. In particular, our results and simulations suggest that enhanced hamstring activity during late swing, rather than early stance, is a factor to knee flexion during stance. This information is relevant for diagnosing and designing effective treatments for gait abnormalities (e.g., crouch gait) that arise from abnormal hamstring activity.

Chapter 6

Conclusions and Recommendations for Future Work

Chapters 2 through 5 have taken us on a path through the effects of age on center of mass accelerations, the accelerations induced by rectus femoris and vastus lateralis on the hip and knee under highly controlled conditions, and the joint angle changes induced by the biarticular rectus femoris and hamstrings when electrically stimulated about the points of their normal activity during walking. In doing so, we have considered the implications of our studies to the gaits of older adults, impaired children (in the case of cerebral palsy) and impaired young and older adults (in the case of stroke).

We first noted that the differences in lower-extremity joint torque and power patterns

between young and older adult gaits that other groups had previously observed [28-32] are reflected in the ground reaction forces and the work done by the limbs. These measures, which can be obtained from force plate data, may one day allow us to determine if these aging tendencies on walking are present in specific subjects. The main differences observed on ground reactions were decreased vertical, forward, and medial accelerations during double support and increased work done on the center of mass during midstance, all of which become amplified during fast walking. Work still needs to be done to establish whether or not a metric can be developed that would provide levels of sensitivity and specificity at least comparable to those offered by McGibbon and Krebs, which required inverse kinematics and dynamics analyses [31].

During our analysis of the accelerations induced by the rectus femoris and vastus lateralis on lower limb segments at postures representative of the early swing phase, we reached three important conclusions; first, that the biarticular rectus femoris extended the hip (not flexed it) and knee if stimulated at a posture corresponding to toe-off; second, that the hip-to-knee acceleration ratios observed roughly matched model-based predictions; and third, that superposition was a reasonable assumption to determine the effects of these two muscles acting together. This study showed that it was indeed possible to measure joint angle

changes resulting from the electrical stimulation of muscles, and that we could use them as a test for the predictions reached via dynamic models.

The logical extension of the new electrical stimulation methodology was to apply it during a dynamic movement, and see whether or not it was still useful. An additional goal was to move from speaking about induced accelerations only to considering the ensuing joint angle changes, because this is a more clinically relevant measure. An important consideration here is that the muscle forces that induce accelerations on the segments need some time before they can generate angular displacements. We asked ourselves whether or not we could still come up with a valid methodology, especially since angular displacements can induce forces in other muscles both due to passive stretch and evoked reflex responses [93]. We reached a compromise by allowing just enough time (300 ms) to reach points of clinical relevance for the specific muscles of interest (i.e., peak knee flexion during swing for rectus femoris activity and peak knee flexion during stance for semitendinosus activity).

Our choice of comparing muscle activities during the 0-150 ms and the 150-300 ms windows following the stimulus seems reasonable but is limited in the sense that the electromyographic traces of normal muscle activity and of stimulated muscles are different and it is not well-known how one relates to the other. In particular, the recruitment of motor

fibers is different in each case, with normal muscle activity recruiting fibers more evenly throughout the muscle than during stimulations, likely producing more force for an equal EMG amplitude. On the other hand, due to the 150 ms delay between the stimulus onset and the start of the reflex-activity measurement window, these measured reflexes have a much lower chance of contributing to the motion. Furthermore, any small amount of measured activity in non-stimulated muscles (whether real or deriving from cross-talk) during the 0-150 ms stimulation period can easily mask any potential reflexes happening then. Developing a technique for determining the amount of reflex activity occurring *simultaneously* with the stimulus (0-150 ms) may assist us in the future to determine the true extent to which reflexes can play a role in the motions induced by electrical stimulation. Such a procedure could perhaps be based on the content of the EMG signal [94] .

Despite the ambiguity surrounding how to measure reflex responses, the general agreement between the simulation and experimental results in our three electrical stimulation experiments suggests that the magnitude of reflex responses is on average small compared to the activity in the stimulated muscle. Therefore, the technique should continue to be used and developed further. The obvious extension of our work, then, would be to study the dynamic function of other muscles during gait. Our first target should probably be the ankle

plantarflexors, which have received previous attention but are still the subject of debate, due again in part to the non-intuitive predictions of dynamic simulations. These muscles are critical to support and propulsion [12, 13, 47, 86, 95], and have been linked both to the deficits in older adult gait [29, 30, 33] as well as in various gait pathologies [96]. There is also a clear area of opportunity in the evaluation of the whole body movements that are elicited by electrical stimulation of even the same muscles that we studied in this dissertation.

Another area where we could potentially extend our work is in the study of muscle function in individuals with gait pathologies. There is currently a growing body of simulations of pathological cases (stiff-knee gait, crouch gait, stroke) [18, 88, 97] that attribute muscle contributions to specific gait impairments. Most of these studies would benefit from *in vivo* validations that take clinically relevant measures into account, such as peak angle changes or excursions. In addition, it would be possible to study dynamic muscle function in individuals who have undergone tendon transfers or botulinum toxin treatments for gait impairments. Evaluating muscle function before and after treatment may allow us to better asses the outcomes of these medical interventions [98].

Finally, there is great potential for using our protocols to attempt gait rehabilitation using electrical stimulation-assisted treadmill training. The idea here is that one can

repetitively perturb a muscle at a specific point in the gait cycle, then note the chronic gait adaptations that result. This approach can have two variants: in the first one, we can study whether or not over-activity of a muscle during a select portion of the gait cycle induces conditions such as stiff-knee or crouch gait—whether as a direct consequence of the stimulation or indirectly via compensations by other muscles. In the second variant of the experiment, we can start with an individual that has a particular gait impairment (say, stiff-knee gait) and study whether repetitive stimulation of a muscle that is believed to be weak or out-of-phase (say, the gastrocnemius) produces a functional improvement. The idea here would be that the subject may stop performing compensatory actions (say, circumduction) once a lost muscle function has been artificially restored. If that were the case, we would then have a stronger case for strengthening particular muscle groups or even providing new forms of external assistance.

In conclusion, we have introduced an *in vivo* electrical stimulation methodology that can be used to measure dynamic muscle function during normal and pathological gait, and has the potential to be used in rehabilitation. A key feature of our methodology is the ability to control the timing of the perturbation within the gait cycle.

Chapter 7

Key Concepts
and Learnings

There is a potential for this dissertation to influence the way that students, researchers and clinicians think about muscle function. In order for that potential to be realized, a number of key concepts and learnings should be emphasized. In the discussion below, these ideas have been *boldfaced and italicized* as an aid for future reference.

When a muscle exerts force, it generates a distinct moment about each of the joints that it spans, which is proportional to the muscle's moment arm about each joint. This moment is one of several generalized forces acting to accelerate the joint. These generalized forces include other joint moments (due to ligament, musculotendon and distal reaction

forces), centripetal forces, Coriolis forces, gravity, and contact with the environment. Thus, the net acceleration of a joint is the sum of many contributions to acceleration (some positive, some negative). The *dynamic function of a muscle is the contribution of a specific muscle to this net acceleration (or to any other measure of motion) evaluated at specific points along a movement.* Dynamic muscle function may also be defined in terms of the induced motion of a body segment or the overall body center of mass.

Because biarticular muscles act at two joints (a proximal and a distal one), they have two contributions to the acceleration of each of their spanned joints. Consider the proximal joint. The first contribution to the proximal joint's acceleration is due to the moment that the muscle applies there, and this acceleration is always consistent with the anatomy [99]. The second contribution to the proximal joint's acceleration is the less intuitive part, and is due to the joint reaction forces that result from the moment applied about the distal joint. This second contribution can be in direct opposition to the first [2]. It is this dual contribution to a joint's acceleration that makes it possible for the biarticular muscle to accelerate one of its spanned joints in a direction opposite the torque applied there, every time that the latter contribution is opposite in direction and greater in magnitude than the former. When this will actually happen depends on body posture and interactions with the environment.

That a muscle can switch function depending on posture is counter-intuitive to most clinicians, partly because Anatomy textbooks categorize muscles based on their spatial orientation relative to the joints, and not based on measured motions or dynamic models. Biomechanists, on the other hand, are often not surprised by this conclusion, which can be directly predicted from dynamic models. Their lack of surprise is often met with skepticism by clinicians and non-modelers who rightfully observe that *current biomechanical models make many assumptions that have not been thoroughly tested*. Hence, such assumptions may render the models inaccurate or even invalid. Part of the motivation for this work was to thus provide *in vivo* data to directly test model predictions.

The general definition of dynamic muscle function offered above allows for various characteristics of the motion to be used in assessing function. One such characteristic could be the joint accelerations generated by muscle activity. However, *induced accelerations are instantaneous and cannot reveal the changes that take place in the ensuing joint angle trajectories*, which are often more clinically relevant. On the other hand, substantial joint angle changes need time to take place. As the accelerations cause changes in angular velocity, which in turn cause changes in angular position, *the forces that other musculotendons exert on the segments can change due to stretch (force-length and*

force-velocity relationships) and variation in moment arms with posture. Consider, for example, the case of a subject with a strong hip flexion contracture. Using induced acceleration analysis, which looks at the contributions of a single muscle to the net instantaneous acceleration of a joint, we may conclude that the RF acts to extend the hip if active during pre-swing. However, the strong hip flexion contracture could very well keep the hip from extending under the influence of RF force. Therefore, had the accelerations been integrated forward to yield induced positions (say, with the hip flexion contracture modeled as an unusually high stiffness in the uniarticular hip flexors) the same model could have predicted an insignificant amount of hip extension for the same perturbation used in the induced acceleration analysis. In this example, the more clinically-relevant conclusion is the one reached via the induced position analysis.

In this dissertation, we therefore looked at **induced position changes, which take both the delays in movement production and the evolving state of the system into account.** The points where the induced position changes were evaluated had clinical relevance, and the muscle activity preceded those points generally by 100-200 ms. We also inferred the direction of the induced acceleration by making sure that the joint angle changes were in the same direction that the trajectories first deviated from their expected paths—except for the

hip angle changes during ST stimulation at 90%GC, which were often transitory, becoming reduced to nearly zero by the time the measurement was made. Our approach thus allowed us to speak about the effect of stimulating a muscle on clinically-relevant measures and not about the muscle's relative potential to accelerate a joint. As a result, we can conclude that "electrical stimulation of the rectus femoris during pre-swing limits peak knee flexion during swing (with a corresponding reduction in hip flexion)" and "electrical stimulation of the semitendinosus during terminal stance increases peak knee flexion during stance" in healthy young adults. It is our belief that these results represent to a great extent the effect that one would see if these muscles were over-active during the same periods that we perturbed them in the simulations (or stimulated them, during the *in vivo* experiments).

There are several clinical implications of our results. We found that the ***RF can limit knee flexion during swing, more so if active during pre-swing than during early swing.*** Therefore, RF overactivity during pre-swing may be contributing to stiff-knee gait. The ***RF also appears to be a hip extensor, not flexor, at the point when it is normally active (stance-to-swing transition).*** Thus, if a healthy subject had their RF released distally, the muscle would lose its knee extensor moment as well as its capacity to induce extension at the hip via dynamic coupling. This would mean that, post-operatively, the muscle would be

acting as a hip flexor, now consistent with its anatomical classification! Clinically, a justification for the RF transfer is the maintenance of the muscle's ability to flex the hip [21, 65]. Our results suggest this is not true, since the RF does not normally flex the hip. However, the surgery does create the potential for RF to flex the hip which, in some cases, could be a desirable outcome. Further study is warranted to document whether or not this behavior would be the same in stroke or CP patients with stiff-knee gait, before and after treatment.

Another finding was that *ST activity during terminal swing generates increased knee flexion during stance*. One interpretation of this result in the context of crouch gait is that spasticity causes the lengthening hamstrings to activate early during swing, inducing the crouched posture. Under this interpretation, hamstring spasticity would be a primary impairment. However, an alternative possibility is that early onset of hamstring activity is used by the system in a compensatory fashion for other purposes. In particular, hamstring activity may reduce the amount of braking experienced by the body center of mass during the forward deceleration phase of walking (late loading through midstance), which could be compensating for a reduced ability to push-off by the opposite limb. In this scenario, the hamstrings could be compensating for neuromuscular impairments elsewhere. It is

interesting that older adults seem to show this compensatory mechanism of reduced plantar flexor push off power [32], accompanied with increased hamstring activity on the opposite limb [90] and less deceleration in early stance [100]. Further research must take place to clarify the extent to which hamstrings overactivity is an impairment or a compensation in CP gait.

Our RF and ST learnings illustrate an important concept that is not new but is often ignored by investigators when thinking about the potential for muscles to generate motion: *the position changes that result from increasing the excitation level to a muscle depend on delays in activation, contraction and skeletal dynamics and in how other system components (e.g., other musculotendons) respond to induced accelerations*. Therefore, when considering a muscle's contribution to a movement, it is at least as important to look at the induced positions as it is to look at the induced accelerations. If induced accelerations are to be used, one must somehow account for the delays present in movement production before interpreting the results. It is my opinion that this can be challenging in the context of clinically assessing the causes of movement disorders.

The experimental methodology that we have introduced provides a framework for a new understanding of dynamic muscle function, one that is based on a consideration of the

in vivo position (e.g., joint angle) changes induced by electrical stimulation of the muscles at points of interest within the gait cycle. This experimental approach provides answers that are clinically relevant and can also be used to validate the predictions of perturbed forward dynamic simulations. Furthermore, the approach is not limited to joint angle changes but can be extended to include segment and/or body center of mass movements. It can be used to study muscle function in normal and pathological gait, as well as following chronic stimulation—which may reveal neural adaptations in chronic diseases. As we move into the future, we hope that more muscles will be studied both *in vivo* and through *in vivo*-validated forward dynamic simulations, such that we can make firm progress in our understanding of dynamic muscle functions. We firmly believe that such improved understanding will be the key to developing more effective treatments for gait impairments.

Bibliography

[1]   Pope MH. Giovanni Alfonso Borelli-The Father of Biomechanics. Spine 2005; 30: 2350-2355.

[2]   Zajac FE, Gordon ME. Determining muscle's force and action in multi-articular movement. Exerc Sport Sci Rev 1989; 17: 187-230.

[3]   Zajac FE, Neptune RR, Kautz SA. Biomechanics and muscle coordination of human walking Part I: Introduction to concepts, power transfer, dynamics and simulations. Gait Posture 2002; 16: 215-232.

[4]   Schwartz M, Lakin G. The effect of tibial torsion on the dynamic function of the soleus during gait. Gait Posture 2003; 17: 113-8.

[5]   Delp SL, Loan JP, Hoy MG, Zajac FE, Topp EL, Rosen JM. An interactive graphics-based model of the lower extremity to study orthopaedic surgical procedures. IEEE Trans Biomed Eng 1990; 37: 757-67.

[6]   Erdemir A, McLean S, Herzog W, van den Bogert AJ. Model-based estimation of muscle forces exerted during movements. Clin Biomech (Bristol, Avon) 2007; 22: 131-54.

[7]   Thelen DG, Anderson FC, Delp SL. Generating dynamic simulations of movement using computed muscle control. J Biomech 2003; 36: 321-328.

[8]   Riley PO, Kerrigan D. Kinetics of stiff-legged gait: induced acceleration analysis. IEEE Trans Rehabil Eng 1999; 7: 420-426.

[9]   Anderson FC, Goldberg SR, Pandy MG, Delp SL. Contributions of muscle forces and toe-off kinematics to peak knee flexion during the swing phase of normal gait:

an induced position analysis. J Biomech 2004; 37: 731-7.

[10] Piazza SJ, Delp SL. The influence of muscles on knee flexion during the swing phase of gait. J Biomech 1996; 29: 723-733.

[11] Kepple TM, Siegel KL, Stanhope SJ. Relative contributions of the lower extremity joint moments to forward progression and support during gait. Gait Posture 1997; 6: 1-8.

[12] Neptune RR, Kautz SA, Zajac FE. Contributions of the individual ankle plantar flexors to support, forward progression and swing initiation during walking. J Biomech 2001; 34: 1387-1398.

[13] Anderson FC, Pandy MG. Individual muscle contributions to support in normal walking. Gait Posture 2002; 17: 159-169.

[14] Jonkers I, Stewart C, Spaepen A. The complementary role of the plantarflexors, hamstrings and gluteus maximus in the control of stance limb stability during gait. Gait Posture 2003; 17: 264-72.

[15] Riley PO, Kerrigan DC. Torque action of two-joint muscles in the swing period of stiff-legged gait: a forward dynamic model analysis. J Biomech 1998; 31: 835-40.

[16] Goldberg SR, Ounpuu S, Delp SL. The importance of swing-phase initial conditions in stiff-knee gait. J Biomech 2003; 36: 1111-6.

[17] Arnold AS, Anderson FC, Pandy MG, Delp SL. Muscular contributions to hip and knee extension during the single limb stance phase of normal gait: a framework for investigating the causes of crouch gait. J Biomech 2005; 38: 2181-9.

[18] Higginson JS, Zajac FE, Neptune RR, Kautz SA, Delp SL. Muscle contributions to support during gait in an individual with post-stroke hemiparesis. J Biomech 2006; 39: 1769-1777.

[19] Chen G. Induced acceleration contributions to locomotion dynamics are not physically well defined. Gait Posture 2006; 23: 37-44.

[20] Kuo AD, Maxwell Donelan J. Comment on "Contributions of the individual ankle plantar flexors to support, forward progression and swing initiation during walking" and "Muscle mechanical work requirements during normal walking: The energetic cost of raising the body's center-of-mass is significant". J Biomech; In Press, Corrected Proof.

[21] Gage JR, Perry J, Hicks RR, Koop S, Werntz JR. Rectus femoris transfer to improve knee function of children with cerebral palsy. Dev Med Child Neurol 1987; 29: 159-66.

[22] El O, Peker O, Kosay C, Iyilikci L, Bozan O, Berk H. Botulinum toxin A injection for spasticity in diplegic-type cerebral palsy. J Child Neurol 2006; 21: 1009-12.

[23] Robertson JVG, Pradon D, Bensmail D, Fermanian C, Bussel B, Roche N. Relevance of botulinum toxin injection and nerve block of rectus femoris to kinematic and functional parameters of stiff knee gait in hemiplegic adults. Gait Posture 2009; 29: 108-112.

[24] Riewald SA, Delp SL. The action of the rectus femoris muscle following distal tendon transfer: does it generate knee flexion moment? Dev Med Child Neurol 1997; 39: 99-105.

[25] Yaraskavitch M, Leonard T, Herzog W. Botox produces functional weakness in non-injected muscles adjacent to the target muscle. J Biomech 2008; 41: 897-902.

[26] Hernandez A, Dhaher Y, Thelen DG. In vivo measurement of dynamic rectus femoris function at postures representative of early swing phase. J Biomech 2008; 41: 137-44.

[27] Delp SL, Loan JP, Hoy MG, Zajac FE, Topp EL, Rosen JM. An interactive graphics-based model of the lower extremity to study orthopaedic surgical procedures. IEEE Trans Biomed Eng 1990; 37: 757-67.

[28] Winter DA, Patla A, Frank J, Walt S. Biomechanical walking pattern changes in the fit and healthy elderly. Phys Ther 1990; 70: 340-347.

[29] Judge JO, Davis R, Ounpuu S. Step length reductions in advanced age: the role of ankle and hip kinetics. J Gerontol A Biol Sci Med Sci 1996; 51: M303-M312.

[30] DeVita P, Hortobagyi T. Age causes a redistribution of joint torques and powers during gait. J Appl Physiol 2000; 88: 1804-1811.

[31] McGibbon CA, Krebs DE. Discriminating age and disability effects in locomotion: neuromuscular adaptations in musculoskeletal pathology. J Appl Physiol 2004; 96: 149-60.

[32] Silder A, Heiderscheit B, Thelen DG. Active and passive contributions to joint kinetics during walking in older adults. J Biomech 2008; 41: 1520-1527.

[33] Kerrigan D, Todd M, Della Croce U, Lipsitz L, Collins J. Biomechanical gait alterations independent of speed in the healthy elderly: evidence for specific limiting impairments. Arch Phys Med Rehabil 1998; 79: 317-322.

[34] Maki BE. Gait changes in older adults: predictors of falls or indicators of fear. J Am Geriatr Soc 1997; 45: 313-20.

[35] Maki BE, McIlroy WE. Control of compensatory stepping reactions: Age-related impairment and the potential for remedial intervention. Physiother Theory Pract 1998: 69-90.

[36] Rogers MW, Mille ML. Lateral stability and falls in older people. Exerc Sport Sci Rev 2003; 31: 182-7.

[37] Bauby CE, Kuo, A. D. Active control of lateral balance in human walking. J Biomech 2000; 33: 1433-1440.

[38] Zajac FE. Muscle and tendon: properties, models, scaling and application to biomechanics and motor control. Crit Rev Biomed Eng 1989; 17: 359-411.

[39] Ivanenko YP, Poppele RE, Lacquaniti F. Five basic muscle activation patterns account for muscle activity during human locomotion. J Physiol 2004; 556: 267-82.

[40] Cappozzo A, Catani F, Croce UD, Leardini A. Position and orientation in space of

bones during movement: anatomical frame definition and determination. Clin Biomech (Bristol, Avon) 1995; 10: 171-178.

[41]   Gard SA, Miff SC, Kuo AD. Comparison of kinematic and kinetic methods for computing the vertical motion of the body center of mass during walking. Hum Mov Sci 2004; 22: 597-610.

[42]   Donelan JM, Kram R, Kuo AD. Simultaneous positive and negative external mechanical work in human walking. J Biomech 2002; 35: 117-24.

[43]   Ortega JD, Farley CT. Individual limb work does not explain the greater metabolic cost of walking in elderly adults. J Appl Physiol 2007; 102: 2266-73.

[44]   Pai YC, Patton J. Center of mass velocity-position predictions for balance control. J Biomech 1997; 30: 347-354.

[45]   Winter DA. Human balance and posture control during standing and walking. Gait Posture 1995; 3: 193-214.

[46]   Goldberg SR, Anderson FC, Pandy MG, Delp SL. Muscles that influence knee flexion velocity in double support: implications for stiff-knee gait. J Biomech 2004; 37: 1189-96.

[47]   Kimmel SA, Schwartz MH. A baseline of dynamic muscle function during gait. Gait Posture 2006; 23: 211-21.

[48]   Zajac FE, Gordon ME. Determining muscle's force and action in multi-articular movement. Exerc Sport Sci Rev 1989; 17: 187-230.

[49]   Piazza SJ. Muscle-driven forward dynamic simulations for the study of normal and pathological gait. J Neuroeng Rehabil 2006; 3: 5.

[50]   Maas H, Baan GC, Huijing PA. Muscle force is determined also by muscle relative position: isolated effects. J Biomech 2004; 37: 99-110.

[51]   Yamaguchi GT, Zajac FE. A planar model of the knee joint to characterize the knee extensor mechanism. J Biomech 1989; 22: 1-10.

[52]   Liu W, Nigg BM. A mechanical model to determine the influence of masses and mass distribution on the impact force during running. J Biomech 2000; 33: 219-24.

[53]   Perry J. Gait Analysis: Normal and Pathological Function. Thorofare, NJ: Slack Incorporated, 1992.

[54]   Perotto A. Anatomical Guide for the Electromyographer: The Limbs and Trunk. 3rd ed. Springfield, IL: Charles C. Thomas, 1994.

[55]   de Leva P. Adjustments to Zatsiorsky-Seluyanov's segment inertia parameters. J Biomech 1996; 29: 1223-30.

[56]   Piazza SJ, Erdemir A, Okita N, Cavanagh PR. Assessment of the functional method of hip joint center location subject to reduced range of hip motion. J Biomech 2004; 37: 349-56.

[57]   Piazza SJ, Delp SL. The influence of muscles on knee flexion during the swing phase of gait. J Biomech 1996; 29: 723-33.

[58]   Delp SL, Loan JP. A computational framework for simulation and analysis of human and animal movement. IEEE Comput Sci Eng 2000; 2: 46-55.

[59]   Neptune RR, Kautz SA, Zajac FE. Contributions of the individual ankle·plantar flexors to support, forward progression and swing initiation during walking. J Biomech 2001; 34: 1387-1398.

[60]   Anderson FC, Pandy MG. A dynamic optimization solution for vertical jumping in three dimensions. Comput Methods Biomech Biomed Engin 1999; 2: 201-231.

[61]   Zhang LQ, Nuber GW. Moment distribution among human elbow extensor muscles during isometric and submaximal extension. J Biomech 2000; 33: 145-54.

[62]   Zajac FE, Neptune RR, Kautz SA. Biomechanics and muscle coordination of human walking Part II: lessons from dynamical simulations and clinical implications. Gait Posture 2003; 17: 1-17.

[63]   Winter DA. The biomechanics and motor control of human gait: normal, elderly and

pathological. 2nd ed. Waterloo, Ontario: Waterloo Biomechanics, 1991.

[64] Pinzur MS, Sherman R, DiMonte-Levine P, Trimble J. Gait changes in adult onset hemiplegia. Am J Phys Med 1987; 66: 228-37.

[65] Perry J. Distal rectus femoris transfer. Dev Med Child Neurol 1987; 29: 153-8.

[66] Goldberg SR, Ounpuu S, Arnold AS, Gage JR, Delp SL. Kinematic and kinetic factors that correlate with improved knee flexion following treatment for stiff-knee gait. J Biomech 2006; 39: 689-98.

[67] Reinbolt JA, Fox MD, Arnold AS, Ounpuu S, Delp SL. Importance of preswing rectus femoris activity in stiff-knee gait. J Biomech 2008; 41: 2362-9.

[68] Winters TF, Jr., Gage JR, Hicks R. Gait patterns in spastic hemiplegia in children and young adults. J Bone Joint Surg Am 1987; 69: 437-41.

[69] Stewart C, Postans N, Schwartz MH, Rozumalski A, Roberts AP. An investigation of the action of the hamstring muscles during standing in crouch using functional electrical stimulation (FES). Gait Posture 2008; 28: 372-7.

[70] Hunter BV, Thelen DG, Dhaher YY. A three-dimensional biomechanical evaluation of quadriceps and hamstrings function using electrical stimulation. IEEE Trans Neural Syst Rehabil Eng 2009; 17: 167-75.

[71] Stewart C, Postans N, Schwartz MH, Rozumalski A, Roberts A. An exploration of the function of the triceps surae during normal gait using functional electrical stimulation. Gait Posture 2007; 26: 482-8.

[72] Thelen DG, Anderson FC. Using computed muscle control to generate forward dynamic simulations of human walking from experimental data. J Biomech 2006; 39: 1107-15.

[73] Walker PS, Rovick JS, Robertson DD. The effects of knee brace hinge design and placement on joint mechanics. J Biomech 1988; 21: 965-74.

[74] Lu TW, O'Connor JJ. Bone position estimation from skin marker co-ordinates using

global optimisation with joint constraints. J Biomech 1999; 32: 129-34.

[75]   Heiderscheit BC, Hoerth DM, Chumanov ES, Swanson SC, Thelen BJ, Thelen DG. Identifying the time of occurrence of a hamstring strain injuring during treadmill running: a case study. Clin Biomech 2005; 20: 1072-8.

[76]   Thelen DG. Adjustment of muscle mechanics model parameters to simulate dynamic contractions in older adults. J Biomech Eng 2003; 125: 70-7.

[77]   Zajac FE. Muscle and tendon: properties, models, scaling, and application to biomechanics and motor control. Crit Rev Biomed Eng 1989; 17: 359-411.

[78]   Crowninshield RD, Brand RA. A physiologically based criterion of muscle force prediction in locomotion. J Biomech 1981; 14: 793-801.

[79]   Arnold AS, Thelen DG, Schwartz MH, Anderson FC, Delp SL. Muscular coordination of knee motion during the terminal swing phase of normal gait. J Biomech 2007; 40: 3314-24.

[80]   Reinbolt JA, Fox MD, Schwartz MH, Delp SL. Predicting outcomes of rectus femoris transfer surgery. Gait Posture 2009; 30: 100-5.

[81]   Cole GK, van den Bogert AJ, Herzog W, Gerritsen KG. Modelling of force production in skeletal muscle undergoing stretch. J Biomech 1996; 29: 1091-104.

[82]   Rozumalski A, Schwartz MH. Crouch gait patterns defined using k-means cluster analysis are related to underlying clinical pathology. Gait Posture 2009; 30: 155-60.

[83]   Sutherland DH, Davids JR. Common gait abnormalities of the knee in cerebral palsy. Clin Orthop Relat Res 1993: 139-47.

[84]   Arnold AS, Thelen DG, Schwartz MH, Anderson FC, Delp SL. Muscular coordination of knee motion during the terminal-swing phase of normal gait. J Biomech 2007; 40: 3314-24.

[85]   Arnold AS, Liu MQ, Schwartz MH, Ounpuu S, Dias LS, Delp SL. Do the hamstrings operate at increased muscle-tendon lengths and velocities after surgical

lengthening? J Biomech 2006; 39: 1498-506.

[86] Neptune RR, Zajac FE, Kautz SA. Muscle force redistributes segmental power for body progression during walking. Gait Posture 2004; 19: 194-205.

[87] Stewart C, Postans N, Schwartz MH, Rozumalski A, Roberts A. An exploration of the function of the triceps surae during normal gait using functional electrical stimulation. Gait Posture 2007.

[88] Hicks JL, Schwartz MH, Arnold AS, Delp SL. Crouched postures reduce the capacity of muscles to extend the hip and knee during the single-limb stance phase of gait. J Biomech 2008; 41: 960-7.

[89] Liu MQ, Anderson FC, Schwartz MH, Delp SL. Muscle contributions to support and progression over a range of walking speeds. J Biomech 2008; 41: 3243-52.

[90] Schmitz A, Silder A, Heiderscheit B, Mahoney J, Thelen DG. Differences in lower-extremity muscular activation during walking between healthy older and young adults. J Electromyogr Kinesiol 2008.

[91] DeLuca PA, Ounpuu S, Davis RB, Walsh JH. Effect of hamstring and psoas lengthening on pelvic tilt in patients with spastic diplegic cerebral palsy. J Pediatr Orthop 1998; 18: 712-8.

[92] Ma FY, Selber P, Nattrass GR, Harvey AR, Wolfe R, Graham HK. Lengthening and transfer of hamstrings for a flexion deformity of the knee in children with bilateral cerebral palsy: technique and preliminary results. J Bone Joint Surg Br 2006; 88: 248-54.

[93] Lewek MD, Hornby TG, Dhaher YY, Schmit BD. Prolonged quadriceps activity following imposed hip extension: a neurophysiological mechanism for stiff-knee gait? J Neurophysiol 2007; 98: 3153-62.

[94] LeFever RS, De Luca CJ. A procedure for decomposing the myoelectric signal into its constituent action potentials--Part I: Technique, theory, and implementation. IEEE Trans Biomed Eng 1982; 29: 149-57.

[95] Kepple TM, Lohmann KN, Stanhope SJ. Relative contributions of the lower extremity joint moments to forward progression and support during gait. Gait Posture 1997; 6: 1-8.

[96] Olney SJ, Richards C. Hemiparetic gait following stroke. Part I: Characteristics. Gait Posture 1996; 4: 136-148.

[97] Liu M, Arnold AS, Goldberg SR, et al. Quadriceps force in stance limits knee flexion in swing: insight from a subject-specific simulation of stiff-knee gait. Gait and Clinical Movement Analysis Meeting. Portland, OR, 2005.

[98] Arnold AS, Anderson FC, Liu M, et al. Biomechanical efficacy of treatments for stiff-knee gait: a simulation-based case study. Gait and Clinical Movement Analysis Meeting. Portland, OR, 2005.

[99] Fregly BJ, Zajac FE. A state-space analysis of mechanical energy generation, absorption, and transfer during pedaling. J Biomech 1996; 29: 81-90.

[100] Hernandez A, Silder A, Heiderscheit BC, Thelen DG. Effect of age on center of mass motion during human walking. Gait Posture 2009; 30: 217-22.